TURUN YLIOPISTON JULKAISUJA
ANNALES UNIVERSITATIS TURKUENSIS

SARJA - SER. A I OSA - TOM. 449

ASTRONOMICA - CHEMICA - PHYSICA - MATHEMATICA

Biosynthesis of pyranonaphthoquinone polyketides: characterization of the alnumycin pathway

by

Terhi Oja

TURUN YLIOPISTO
UNIVERSITY OF TURKU
Turku 2012

From the Department of Biochemistry and Food Chemistry
University of Turku, Finland

Supervised by

Mikko Metsä-Ketelä, Ph.D.
Department of Biochemistry and Food Chemistry
University of Turku

Docent Jarmo Niemi, Ph.D.
Department of Biochemistry and Food Chemistry
University of Turku

Professor Emeritus Pekka Mäntsälä, Ph.D.
Department of Biochemistry and Food Chemistry
University of Turku

Reviewed by

Professor Kaarina Sivonen, Ph.D.
Department of Food and Environmental Sciences
University of Helsinki

Docent Tuomo Glumoff, Ph.D.
Department of Biochemistry
University of Oulu

Opponent

Professor Thomas J. Simpson, Ph.D.
School of Chemistry
University of Bristol
United Kingdom

ISBN 978-951-29-5205-2 (PRINT)
ISBN 978-951-29-5206-9 (PDF)
ISSN 0082-7002
Painosalama Oy – Turku, Finland 2012

CONTENTS

ABSTRACT

Alnumycin A is an aromatic pyranonaphthoquinone (PNQ) polyketide closely related to the model compound actinorhodin. While some PNQ polyketides are glycosylated, alnumycin A contains a unique sugar-like dioxane moiety. This unusual structural feature made alnumycin A an interesting research target, since no information was available about its biosynthesis. Thus, the main objective of the thesis work became to identify the steps and the enzymes responsible for the biosynthesis of the dioxane moiety.

Cloning, sequencing and heterologous expression of the complete alnumycin gene cluster from *Streptomyces* sp. CM020 enabled the inactivation of several alnumycin biosynthetic genes and preliminary identification of the gene products responsible for pyran ring formation, quinone formation and dioxane biosynthesis. The individual deletions of the genes resulted in the production of several novel metabolites, which in many cases turned out to be pathway intermediates and could be used for stepwise enzymatic reconstruction of the complete dioxane biosynthetic pathway *in vitro*. Furthermore, the *in vitro* reactions with purified alnumycin biosynthetic enzymes resulted in the production of other novel compounds, both pathway intermediates and side products.

Identification and molecular level studies of the enzymes AlnA and AlnB catalyzing the first step of dioxane biosynthesis – an unusual C-ribosylation step – led to a mechanistic proposal for the C-ribosylation of the polyketide aglycone. The next step on the dioxane biosynthetic pathway was found to be the oxidative conversion of the attached ribose into a highly unusual dioxolane unit by Aln6 belonging to an uncharacterized protein family, which unexpectedly occurred without any apparent cofactors. Finally, the last step of the pathway was found to be catalyzed by the NADPH-dependent reductase Aln4, which is able to catalyze the conversion of the formed dioxolane into a dioxane moiety.

The work presented here and the knowledge gained of the enzymes involved in dioxane biosynthesis enables their use in the rational design of novel compounds containing C–C bound ribose, dioxolane and dioxane moieties.

LIST OF ORIGINAL PUBLICATIONS

This thesis is based on the following publications, referred to as I–IV in the text:

I Oja T., Palmu K., Lehmussola H., Leppäranta O., Hännikäinen K., Niemi J., Mäntsälä P., Metsä-Ketelä M. **(2008)** Characterization of the alnumycin gene cluster reveales unusual gene products for pyran ring formation and dioxan biosynthesis. *Chem. Biol.* **15**, 1046–1057.

II Grocholski T.*, Oja T.*, Humphrey L., Mäntsälä P., Niemi J., Metsä-Ketelä M. **(2012)** Characterization of the two-component monooxygenase system AlnT/AlnH reveals early timing of quinone formation in alnumycin biosynthesis. *J. Bacteriol.* **194**, 2829–2836. * Equal contribution.

III Oja T., Klika K.D., Appassamy L., Sinkkonen J., Mäntsälä P., Niemi J., Metsä-Ketelä M. **(2012)** Biosynthetic pathway toward carbohydrate-like moieties of alnumycins contains unusual steps for C–C bond formation and cleavage. *Proc. Natl. Acad. Sci. U. S. A*. **109**, 6024–6029.

IV Oja T.*, Niiranen L.*, Sandalova T., Klika K.D., Niemi J., Mäntsälä P., Schneider G., Metsä-Ketelä M. **(2012)** Structural basis for C-ribosylation in the alnumycin A biosynthetic pathway. * Equal contribution. (Submitted.)

The original publications I–III were reproduced with permissions from the copyright holders. In addition to the publications I–IV, some of the results of the thesis work were included in the following publications:

Oja T., Tähtinen P., Dreiack N., Mäntsälä P., Niemi J., Metsä-Ketelä M., Klika K.D. **(2012)** Alnumycins A2 and A3: new inverse-epimeric pairs stereoisomeric to alnumycin A1. *Tetrahedron: Asymmetry* **23**, 670–682.

Tähtinen P., Oja T., Dreiack N., Mäntsälä P., Niemi J., Metsä-Ketelä M., Klika K.D. **(2012)** Epimers vs. inverse epimers: the C-1 configuration in alnumycin A1. *RSC Adv.* **2**, 5098–5100.

ABBREVIATIONS

aa = amino acid

ACP = acyl carrier protein

CoA = coenzyme A

DHPA = 1,6-dihydroxy-8-propylanthraquinone

DNPA = 4-dihydro-9-hydroxy-1-methyl-10-oxo-3-*H*-naphtho[2,3-*c*]pyran-3-acetic acid

HPLC = high-performance liquid chromatography

KS = ketosynthase, ketoacyl synthase

MAT = malonyl–CoA:ACP transacylase

minPKS = minimal polyketide synthase

NDP = nucleoside diphosphate

NMR = nuclear magnetic resonance

ORF = open reading frame

PCR = polymerase chain reaction

PKS = polyketide synthase

PNQ = pyranonaphthoquinone

1 INTRODUCTION

The soil-dwelling bacterial species of the genus *Streptomyces* are well known for their production of a wide range of antimicrobial compounds. These Gram-positive, filamentous bacteria are saprophytes, and morphologically adapted to life in soil. Their life cycle includes germination of spores, growth of mycelia and formation of aerial hyphae, which later develop into spores, thus completing the cycle. The synthesis of bioactive compounds against competing organisms only occurs under certain nutritional conditions and at a specific growth phase and morphological stage, often as a response to starvation (Bibb 1996, Hopwood 2007).

The importance of *Streptomyces* species as producers of medicinally useful compounds was already recognized in the 1940s, when the first effective treatment against tuberculosis – the aminoglycoside antibiotic streptomycin – was discovered. This discovery, together with an earlier finding of the β-lactam antibiotic penicillin produced by a fungal species, started the era of antibiotics. *Streptomyces* species still continue to be an important source of various medicinally useful compounds and antibiotics in particular; approximately two-thirds of the medicinally used antimicrobial agents are natural products of *Streptomyces* species, or their semisynthetic derivatives (Hopwood 2007).

A major concern related to the use of antibiotics is the ability of the target microbes to develop resistance, which was noticed early on after the first important antibiotics had found medicinal use. Resistance to antibiotics still remains a problem, and it is one of the driving forces in the search for novel biologically active compounds. As *Streptomyces* species and related bacteria have evolved to produce bioactive compounds, they continue to be an important source of potential new drug leads (Bérdy 2012). Knowledge of the antibiotic biosynthetic pathways of *Streptomyces* species and detailed mechanistic understanding of the enzymes catalyzing the biosynthetic steps set the ground for the controlled design of novel natural products.

The thesis work focused on the identification of the biosynthetic enzymes responsible for the formation of a unique dioxane moiety of a type II polyketide alnumycin A. Characterization of the alnumycin biosynthetic pathway involved studies on unusual enzymatic activities and reaction mechanisms encountered during the project, as well as structural analysis of both the biosynthetic enzymes and the novel natural products produced by them.

2 LITERATURE REVIEW

2.1 The polyketide class of natural products

The polyketide class of compounds is one of the major classes of medicinally used secondary metabolites of *Streptomyces* and related species of the order *Actinomycetales*. Important polyketides produced by these species include antibiotics (amphotericin B, erythromycin, rifamycins, tetracyclines), antiparasite drugs (avermectin), anticancer drugs (doxorubicin) and immunosuppressants (rapamycin, tacrolimus) (Hopwood 2007).

Besides *Streptomyces* and closely related species, other bacterial and fungal species and plants produce various polyketides, some of which have less positive effects on human and animal health. Aflatoxins and many other mycotoxins, which cause problems in food safety and agriculture, are actually polyketides produced by fungal species (Huffman *et al.* 2010).

Regardless of the identity of the producing organism, all polyketides share a similar biosynthetic origin closely related to fatty acid biosynthesis. Polyketide biosynthesis is catalyzed by a polyketide synthase (PKS) and involves the decarboxylative condensation of small acyl substrates, often malonyl units, bound to an acyl carrier protein (ACP), into a longer carbon chain in which every second carbon carries an original keto group of the substrate. A fundamental difference between polyketide and fatty acid biosynthesis is the full reduction of the β-keto group of each intermediate during fatty acid synthesis. In bacterial fatty acid synthesis, this is catalyzed by separate enzymes responsible for β-ketoreduction, dehydration and enoyl reduction steps (Keller *et al.* 2005, White *et al.* 2005, Gago *et al.* 2011).

Based on the characteristic features of the polyketide synthases, polyketides have been classified into three main categories. Type I synthases are large, multifunctional megasynthases analogous to eukaryotic type I fatty acid synthases, where multiple biosynthetic reactions are catalyzed by individual domains within a single polypeptide (Smith & Tsai 2007). While bacterial type I megasynthases consist of a separate module for each (methyl)malonyl addition, fungal type I systems are limited to a set of domains within one module, which is used in a repetitive manner – thus the name "iterative" PKSs (Keller *et al.* 2005).

Type II PKSs, on the other hand, are analogous to type II fatty acid synthases found in most bacteria, mitochondria and chloroplasts, as their polyketide product is synthesized by a number of monofunctional enzymes, which all catalyze different biosynthetic reactions one after another (White *et al*. 2005). A so-called minimal polyketide synthase (minPKS) complex consisting of three enzymes catalyzes the iterative condensation of acyl units into a long polyketide chain, which is subsequently folded and modified into a final polyketide backbone by dedicated enzymes like cyclases, ketoreductases

and oxygenases (Schneider 2005, Zhou *et al.* 2010). Examples of type II or "aromatic" polyketides in clinical use are the anthracyclines doxorubicin and aclacinomycin A used in the treatment of cancer, and oxytetracycline and tetracenomycin used as antibiotics (Fig. 1, Schneider 2005). In addition to anthracyclines, tetracyclines and tetracenomycins, important subclasses of type II polyketides include: angucyclines (Kharel & Rohr 2012); aureolic acids (O'Connor 2004); compounds of the pluramycin group (Sun *et al*. 1993); compounds of the pradimicin type (Xu *et al*. 2007); pyranonaphthoquinones (PNQs, Brimble *et al.* 1999, Salaski *et al*. 2009), which are often referred to as benzoisochromanequinones (BIQs); and rubromycins (Yunt *et al*. 2009). Each of these compound classes is defined by the presence of characteristic structural features.

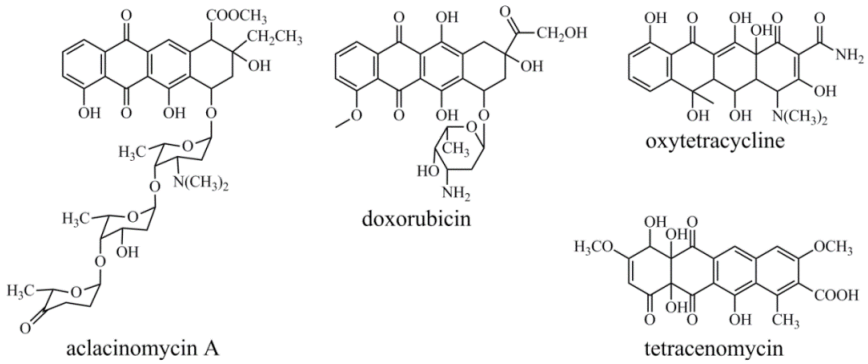

Figure 1. Structures of type II polyketides in clinical use.

The multidomain type III PKSs found in both bacteria and plants resemble the type I enzymes, although they are simpler in their architecture. The homodimeric type III synthases are smaller than the type I megasynthases and lack one of the central domains: the ACP domain. For this reason, type III synthases catalyze the condensation of diverse coenzyme A (CoA)-derivatized substrates rather than the typical ACP-bound small substrates of the other polyketide synthases (Gross *et al.* 2006, Watanabe *et al*. 2007).

Many polyketides – including medicinally useful ones – are glycosylated, and in several cases the sugar moieties have been shown to be important for the biological activities of these compounds (Weymouth-Wilson 1997, Kren & Martínková 2001). Glycosylation of polyketides typically requires the activation of a sugar by a nucleotidyltransferase, which catalyzes the coupling of a sugar-1-phosphate to a nucleoside monophosphate unit of a nucleoside triphosphate. The formed nucleoside diphosphate (NDP)-sugar, often an NDP-D-glucose, is then enzymatically modified and finally attached to the polyketide backbone by a glycosyltransferase, most often via an O-glycosidic bond (Thibodeaux *et al.* 2007). C-glycosidic bonds – which are hydrolytically more stable – are considered less common, although there are several examples of C-glycosylated polyketides (Hultin 2005).

2.2 The structures and biological activities of the PNQ polyketides produced by *Streptomyces* species

A common structural nominator of compounds belonging to the PNQ subclass of type II polyketides is a fused, relatively planar 3-ring structure composed of a pyran, a quinone and a benzene ring (Brimble *et al.* 1999, Salaski *et al*. 2009). The presence of the quinone ring explains the pH-indicator property of pyranonaphthoquinones; the red and yellow compounds turn blue or purple in alkaline conditions (Takano *et al.* 1976). The *p*-quinone is most often found as the central ring, like in the model compound actinorhodin, but in alnumycin A it has an atypical position as a lateral ring. The aglycone structures also differ in the pattern of oxygenation, as only actinorhodin, alnumycin A and granaticin are oxygenated at C-8 (reversed biosynthetic numbering: the carbons of the unfolded polyketide chain are numbered starting from the terminal carboxylic acid carbon). The terminal carboxylic acid, which is not present in alnumycin A, is often found in a cyclized γ-lactone form. Curiously, while none of the PNQ polyketides are directly O-glycosylated, both granaticin and medermycin are C-glycosylated (Fig. 2).

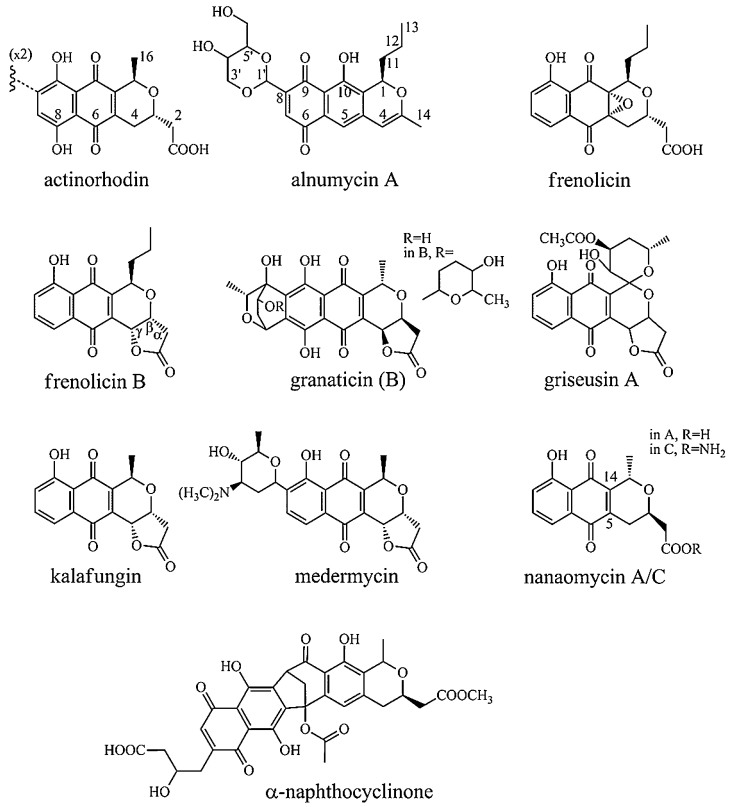

Figure 2. Structures of representative PNQ polyketides and the PNQ-like natural product α-naphthocyclinone. Reversed biosynthetic numbering (actinorhodin and nanaomycins), carbon numbering for alnumycin A and nomenclature for lactone ring carbons (frenolicin B) are shown.

The model compound actinorhodin produced by *Streptomyces coelicolor* A3(2) has an atypical dimeric structure, where two identical units are coupled via a C_{10}–C_{10} bond (Fig. 2). Actinorhodin was reported to only have low antibiotic activity against Gram-positive species, which is possibly compensated by the relatively high production levels of actinorhodin observed for *S. coelicolor* A3(2) (Wright & Hopwood 1976).

Alnumycin A was isolated in 1998 from both *Streptomyces* sp. DSM 11575 (Bieber *et al.*. 1998) and *Streptomyces griseorubiginosus* strain Mer-K1115, under the name K1115 B_1 (Naruse *et al.* 1998). The non-glycosylated alnumycin A is an exceptional member of the PNQ class in having a unique sugar-like 4'-hydroxy-5'-hydroxymethyl-2',7'-dioxane moiety attached via a C–C bond to the polyketide backbone (Bieber *et al.* 1998, Naruse *et al.* 1998, Fig. 2). Very recently, stereochemical analysis of alnumycin A isolated from cultures of *Streptomyces* sp. CM020 revealed exceptionally complex stereochemistry for the compound. Alnumycin A was found to be produced as three pairs of stereoisomers, one of which consisted of previously reported compounds with a (1*R*, 1′*RS*, 4′*RS*, 5′*SR*) configuration (Tatsuta *et al.* 2011, Tähtinen *et al.* 2012). The plausible configurations of the two novel pairs of stereoisomers were (1*R*, 1′*RS*, 4′*SR*, 5′*SR*) and (1*R*, 1′*RS*, 4′*SR*, 5′*RS*) (Oja *et al.* 2012). The biological activities reported for alnumycin A include antibacterial activity against Gram-positive species and cytostatic activity against human leukemia cells, as well as inhibitory activity against gyrase and topoisomerases 1 and 2 (Bieber *et al*. 1998, Björn & Jörg 1998).

Frenolicin, originally isolated from cultures of *Streptomyces fradiae*, can be easily converted to deoxyfrenolicin by chemical reduction of the epoxide (Ellestad *et al*.1968). Chemical oxidation of deoxyfrenolicin, on the other hand, leads to the formation of its γ-lactone derivative frenolicin B (Fig. 2, Fitzgerald *et al.* 2011a). Both deoxyfrenolicin and frenolicin B were isolated from *Streptomyces roseofulvus* strain AM-3867, and they showed promising antimicrobial activity against fungi and mycoplasma (Iwai *et al.* 1978). Other reported activities of frenolicin B include strong inhibition of platelet aggregation, compared to deoxyfrenolicin and other selected naphthoquinones (Nakagawa *et al.* 1987), and anticoccidial activity against the parasite *Eimeria tenella* in chickens. In the latter case, the presence of the γ-lactone ring was suggested to be important for the high antiparasite activity (Omura *et al.* 1985). Frenolicin B was also found to possess moderate *in vitro* activity against human malarial pathogen *Plasmodium falciparum* and to be well tolerated, with no acute toxicity in rats (Fitzgerald *et al.* 2011a). Recently, both deoxyfrenolicin and frenolicin B were recognized as promising anticancer compounds, possibly owing to their selective kinase inhibitory activity against a serine-threonine kinase AKT, which is known to be constitutively activated in a wide variety of human tumor types. A similar inhibitory effect was observed for kalafungin and medermycin, and the PNQ compounds were proposed to act via an S-alkylation mechanism of a

cysteine residue, involving the reduction of the quinone ring to a hydroquinone and subsequent opening of the γ-lactone ring (Toral-Barza *et al.* 2007, Salaski *et al.* 2009).

The granaticin producing strain *Streptomyces violaceoruber* Tü22 produces several related granaticins, which contain a 2,6-dideoxy-D-glucose moiety connected to the aglycone in a highly unusual manner via two C–C bonds, thus forming an additional, fourth fused ring. Both granaticin B and the non-lactone form dihydrogranaticin B are even O-glycosylated, but only indirectly at one of the hydroxyl groups of the first sugar moiety (Fig. 2, Ichinose *et al.* 1998). The reported biological activities of granaticin include antibiotic activity against Gram-positive bacteria (Hultin 2005), cytotoxicity against human oral epidermoid carcinoma (KB) cells (Heinstein 1982) and an inhibitory effect on pyruvate decarboxylase (Gibson-Clay *et al*. 1982). Additionally, also granaticin B was found to be active against Gram-positive bacteria, and to inhibit the growth of transplanted tumors in rodent models (Hultin 2005).

Griseusins A and B, synthesized by a type II polyketide synthase of *Streptomyces griseus* K-63 (Yu *et al.* 1994), only differ in the former being a γ-lactone and the latter a non-lactone form. Both were reported to have potent antibacterial activity against Gram-positive species (Tsuji *et al.* 1976).

Contrary to the weak antibacterial activity observed for actinorhodin, its biosynthetic intermediate kalafungin (Fig. 2), first isolated from *Streptomyces tanashiensis* strain Kala UC-5063 (Cole *et al.* 1987), was shown to have relatively wide-spectrum antibacterial activity, as well as potent activity against a variety of pathogenic fungi, yeasts and protozoa (Johnson & Dietz 1968). Interestingly, the antibacterial properties of kalafungin were reported to be very similar to its enantiomer nanaomycin D, indicating that in this case the stereochemistry of the compound would not significantly affect its biological activity (Tatsuta *et al.* 1991).

Medermycin, also referred to as natural lactoquinomycin (Tatsuta *et al.* 1990, Hultin 2005), was isolated from cultures of *S. tanashiensis* K73 (Takano *et al*. 1976). The compound was found to be C-glycosylated with a glucose-derived angolosamine moiety (Ichnose *et al.* 2003). Medermycin was reported to show promising antibacterial activity against Gram-positive species, including resistant *Staphylococcus aureus* strains (Takano *et al.* 1976, Tatsuta *et al*. 1991), inhibition of platelet aggregation (Nakagawa *et al.* 1987), activity against Ehrlich carcinoma in mice, and cytotoxicity against leukemia and lymphoblastoma cell lines (Tanaka *et al*. 1985, Hultin 2005). Analogously to kalafungin and its enantiomer, the natural (+)-medermycin was found to exhibit similar antibacterial activity as its unnatural enantiomer, suggesting that the stereochemistry of the lactone ring or the C-glycoside is not important for its antibiotic activity (Tatsuta *et al*. 1991).

Nanaomycins A, B, C, D and E were isolated from cultures of *Streptomyces rosa* var. *notoensis*, and their polyketide origin was verified by feeding experiments using labeled 1-^{13}C-acetate (Tanaka *et al.* 1975a, Kasai *et al.* 1979). Rather curiously, it was found that the nanaomycin producing strain also produces frenolicin and similarly, the frenolicin B producing *S. roseofulvus* AM-3867 produces nanaomycin A (Tsuzuki *et al.* 1986). The structure of nanaomycin B differs from other nanaomycins in being hydroxylated at position 14, thus lacking the typical double bond between carbons 5 and 14 (Fig. 2, Tanaka *et al.* 1975b), which is also missing from a frenolicin-like epoxy derivative of nanaomycin A, nanaomycin E (Kasai *et al.* 1979). The γ-lactone form nanaomycin D is likely to be a biosynthetic intermediate, as it could be converted to nanaomycin A *in vitro* through either enzymatic or chemical reduction of the quinone, which was proposed to lead to lactone ring opening via intramolecular electron transfer from the hydroquinone product (Tanaka *et al.* 1982). The comparison of biological activities of nanaomycins A–C to activities of several derivatives indicated that presence of the phenolic hydroxyl group is important for the observed antimicrobial activity against Gram-positive bacteria, fungi and mycoplasma (Tanaka *et al.* 1975c). Recently, nanaomycin A was reported to selectively inhibit human DNA methyltransferase 3B leading to the reactivation of silenced tumor suppressor genes in human cancer cells (Kuck *et al.* 2010).

A dimeric PNQ-like compound α-naphthocyclinone lacking a complete quinone ring was isolated from cultures of *Streptomyces arenae* DSM 40737 (Zeeck & Mardin 1974), and the polyketide origin of the compound was confirmed by gene inactivation and heterologous expression experiments (Brünker *et al.* 1999). Different oxygenation and cyclization patterns were observed for the two units, which are fused via two C–C bonds (Zeeck & Mardin 1974). Intriguingly, α-naphthocyclinone is another example of a PNQ-type aglycone modified via C–C bond formation, and in all cases the position of one C–C bond is analogous to the position C-10 of actinorhodin (Fig. 2).

2.3 PNQ biosynthetic gene clusters

Type II polyketide biosynthetic genes tend to reside clustered in *Streptomyces* genomes, which enables the analysis and expression of complete biosynthetic clusters cloned as single, large DNA fragments. In addition to the alnumycin cluster characterized in this study, complete biosynthetic gene clusters have been cloned, sequenced and heterologously expressed for three PNQ polyketides: the actinorhodin gene cluster from *S. coelicolor* A3(2) (Malpartida & Hopwood 1984), the granaticin gene cluster from *S. violaceoruber* Tü22 (Ichinose *et al.* 1998) and the medermycin gene cluster from *S.* sp. AM-7161 (Ichinose *et al*. 2003). Sequence analysis of the gene clusters revealed 22, 37 and 34 ORFs (open reading frames) likely to be involved in the biosynthesis

of actinorhodin, granaticin and medermycin, respectively. Also the frenolicin, griseusin and naphthocyclinone biosynthetic gene clusters from *S. roseofulvus*, *S. griseus* and *S. arenae* have been partially cloned and sequenced (Bibb *et al.* 1994, Yu *et al.* 1994, Brünker *et al.* 1999).

Comparative sequence analysis of the actinorhodin, granaticin and medermycin gene clusters revealed that a high degree of sequence identity was generally found for PKS-stage enzymes involved in the synthesis of the polyketide chain and the closely associated first and second ring cyclization steps. An unexpected finding was the location of the medermycin ACP gene, which was not discovered immediately downstream of the minPKS ketosynthase genes, but instead 20 kbp upstream of them, together with *med-orf24* deduced to code for a holo-ACP synthase. Another curious feature of the medermycin cluster was the presence of an ORF (*med-orf22*) deduced to code for an acyl-CoA carboxyl transferase (Ichinose *et al.* 2003), but the possible role of the gene product in malonyl-CoA formation has not been investigated.

2.4 The early biosynthetic steps of PNQ polyketides

2.4.1 The formation of the polyketide chain by minimal PKS enzymes

The mechanism of polyketide chain formation is fairly well understood, as PNQ ketosynthase (KS) enzymes are homologous to both fatty acid synthases and other polyketide synthases. Together with an ACP, ketosynthase α (KS_α, KS) and ketosynthase β (KS_β, chain length factor, CLF) form the minPKS complex and catalyze the condensation of malonyl units in a decarboxylative manner into a long polyketide chain (Carreras & Khosla 1998).

Polyketide biosynthesis is typically initiated by the decarboxylation of the first ACP-bound malonyl unit (Fig. 3a) catalyzed by the KS, followed by the transfer of the formed acetyl unit to a conserved cysteine residue of the KS. The decarboxylation of the second malonyl-ACP generates a negatively charged acetyl intermediate, which acts as a nucleophile and attacks the carbonyl carbon of the first KS-bound acetyl unit, forming a four-carbon long diketide attached to the ACP. The diketide is then transferred to the conserved cysteine residue of the KS, and the next malonyl-ACP is decarboxylated (Fig. 3b). Similar Claisen condensations between the growing polyketide chain and malonyl-ACP units are repeated until a polyketide product of correct length is formed (Dreier & Khosla 2000, Keatinge-Clay *et al.* 2004).

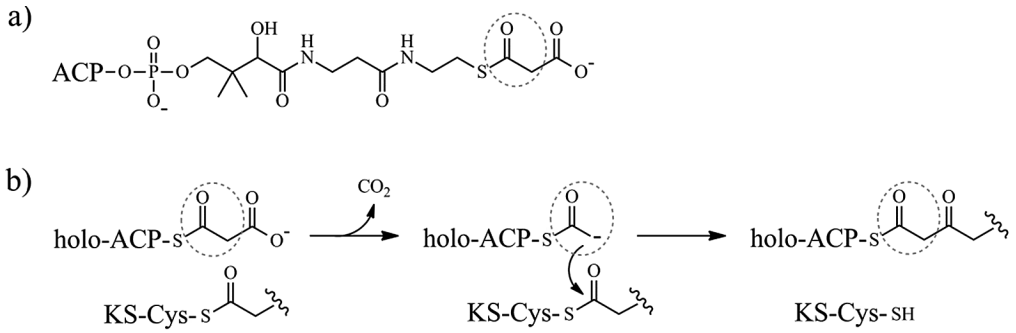

Figure 3. a) The chemical structure of a malonylated phosphopantetheine arm of a holo-ACP. b) A simplified model for the decarboxylative condensation reaction catalyzed by the minPKS. One two-carbon extension unit is circled with a dashed gray line.

Malonyl building blocks for polyketide synthesis are activated by the transfer from malonyl-CoA to an ACP, which is possibly catalyzed by a malonyl–CoA:ACP transacylase (MAT) enzyme shared with fatty acid metabolism (Carreras & Khosla 1998, Gago *et al.* 2011). MAT is able to catalyze the covalent attachment of each malonyl unit as a thioester to a phosphopantetheine arm of a holo-ACP (Fig. 3a), but even self-malonylation of type II holo-ACPs *in vitro* has been reported (Hitchman *et al*. 1998). Thus, it has been suggested that there might be no absolute requirement for a MAT in polyketide biosynthesis (Matharu *et al.* 1998, Arthur *et al*. 2005).

Only holo-ACPs can be malonylated, and the post-translational modification of an apo-ACP is catalyzed by a holo-ACP synthase ("phosphopantetheinyl transferase"). The holo-ACP synthase catalyzes the transfer of a phosphopantetheine chain (Fig. 3a) from CoA to a conserved serine residue of an apo-ACP. Two of the known PNQ gene clusters harbor putative genes for holo-ACP synthases (*med-orf24* and *gra-orf32*, Ichinose *et al.* 2003), although the covalent modification of many type II apo-ACPs might be catalyzed by an enzyme shared with fatty acid biosynthesis. In the actinorhodin producing *S. coelicolor* one of the three deduced holo-ACP synthases, AcpS, was suggested to be essential for fatty acid biosynthesis (Lu *et al.* 2008), and shown *in vitro* to catalyze phosphopantetheinyl transfer to both fatty acid synthase ACP and actinorhodin ACP (Cox *et al.* 2002). Recently, AcpS was reported to bind both apo-ACPs with very similar dissociation constants (Dall'Aglio *et al.* 2011).

It has been proposed that the formed polyketide chain would remain attached to the ACP (Khosla 2009), but the exact timing of the thioester hydrolysis is not known. The solution structure of the actinorhodin ACP revealed that the small four-helix bundle protein exhibits more conformational flexibility than the structurally closely related *Escherichia coli* ACP involved in fatty acid biosynthesis (Evans *et al*. 2009), and the deduced interaction of actinorhodin ACP with the C-9 ketoreductase ActIII has been

modeled (Hadfield *et al*. 2004). However, currently there is no direct experimental evidence for interaction of a type II polyketide ACP with any of the "downstream" enzymes.

Due to high reactivity and possibility of spontaneous, incorrect cyclizations of the polyketide chain, the first cyclization events have proved challenging to dissect from the minPKS catalyzed reactions. The *in vitro* production of polyketides with one correctly cyclized ring, using only minPKS enzymes, a MAT and malonyl-CoA as a substrate, has led to the proposal that the minPKS complex might partially control the first cyclization of the formed polyketide chain (Carreras & Khosla 1998).

The hypothesis that the KS–CLF dimer not only determines the chain length, but also promotes correct first ring cyclization, was supported by the high-resolution structure of the actinorhodin KS–CLF dimer (ActI-Orf1–ActI-Orf2) with bound intermediates. The homologous KS_{α} and CLF were found to share the expected, conserved thiolase fold, and an active site was verified to be created by the relatively large dimer interface. The crystal structure revealed that catalytically important residues are either not conserved or not positioned correctly in the CLF, and highlighted the central catalytic role of KS_{α}. The dimer interface was proposed to determine the length of the active site tunnel, and it was suggested that the growing polyketide chain is forced to bend in order to fit inside the tunnel (Keatinge-Clay *et al.* 2004).

2.4.2 Starter unit synthesis

Actinorhodin minPKS and most other PNQ minPKSs catalyze the decarboxylative condensation of 8 malonyl-ACP units into 16-carbon long polyketide chains, whereas alnumycin and frenolicin are formed from 18-carbon long polyketide chains. Curiously, the same minPKS that is responsible for the production of the 18-carbon long frenolicin can apparently also synthesize the 16-carbon long polyketide nanaomycin (Bibb *et al.* 1994, McDaniel *et al.* 1994). The difference in chain lengths originates from the use of an alternative starter unit in place of an acetyl unit of a malonyl-ACP, and the frenolicin gene cluster harbors genes coding for an additional ketoacyl synthase (FrnI), acyl transferase (FrnK) and a specific ACP (FrnJ) involved in the priming of the polyketide chain synthesis with a longer starter unit (Tang *et al*. 2003).

The homodimeric starter unit ketoacyl synthase FrnI is homologous to the bacterial β-ketoacyl-ACP synthase III (KSIII, FabH), which is known to catalyze the decarboxylative condensation of malonyl-ACP with a priming acyl-CoA at the initiation stage of fatty acid synthesis (White *et al.* 2005). It has been proposed that frenolicin biosynthesis might be initiated in a similar manner, by the decarboxylative

condensation of malonyl-ACP and acetyl-CoA. Subsequent reduction of the β-keto group of the formed diketide, followed by dehydration and reduction steps catalyzed by unidentified enzymes possibly shared with fatty acid biosynthesis, would yield a butyryl-ACP starter unit. The hypothesis was supported by *in vitro* analysis of the priming KS and ACP enzymes; FrnI accepted malonyl-FrnJ and labeled acetyl-CoA as substrates, while malonylated minPKS-ACPs were poor substrates for starter unit synthesis by FrnI. It was concluded that the starter unit and minPKS ACPs seem to be specific for the respective ketosynthases, although several studies have indicated that the minPKS ketosynthases are able to recognize ACPs from different type II polyketide pathways (McDaniel *et al.* 1993, Tang *et al.* 2003). Recently, frenolicin starter unit and minPKS genes were coexpressed in a *Streptomyces* host with several genes encoding actinorhodin downstream enzymes (ActIII, ActIV, ActVII, ActVI-Orf1, ActVI-Orf2 and ActVB), which resulted in the successful production of low levels of deoxyfrenolicin, with butyryl-primed shunt products as the main relevant secondary metabolite products (Fitzgerald *et al.* 2011b).

A similar set of three proteins homologous to frenolicin starter unit enzymes was shown to catalyze starter unit formation in the biosynthesis of a type II polyketide R1128 (Marti *et al.* 2000, Tang *et al.* 2004). The high-resolution crystal structure of the starter unit ketoacyl-ACP synthase ZhuH from *Streptomyces* sp. R1128 was obtained in complex with one of the alternative substrates, acetyl-CoA, and the overall fold of ZhuH was found to be similar to that of FabH from *E. coli* and other priming ketosynthases from fatty acid biosynthetic pathways (Pan *et al.* 2002). Intriguingly, the starter unit acyl transferase ZhuC from the R1128 pathway was proposed to act as a thioesterase, catalyzing the hydrolysis of incorrect acyl groups attached to the starter unit ACP, thereby enabling more efficient priming of the polyketide synthesis with longer starter units, like hexanoyl-ACP (Tang *et al.* 2004).

2.4.3 The first and the second ring cyclizations

On PNQ pathways, the first two ring cyclizations are so intimately linked to ketoreduction at position C-9 that the exact order of these events has proved challenging to determine. Functional studies of the actinorhodin C-9 ketoreductase ActIII revealed that *in vitro* co-incubation of actinorhodin minPKS enzymes with the ketoreductase increased the yield of a shunt product, mutactin, with a correctly cyclized, reduced first ring (Fig. 4). Curiously, another shunt product SEK4, with a correctly cyclized but unreduced first ring (Fig. 4), is produced even without the addition of the ketoreductase (Hadfield *et al.* 2004). This finding, together with the observed high regiospecificity of the C-9 ketoreductases, has supported the hypothesis that already the minPKS might promote the first ring cyclization (Korman *et al.* 2004).

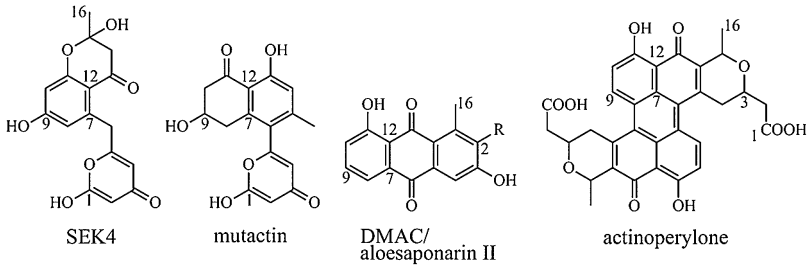

Figure 4. Structures of selected shunt products from the actinorhodin biosynthetic pathway. R = COOH in DMAC (3,8-dihydroxy-1-methylanthraquinone-2-carboxylic acid) and R = H in aloesaponarin II. Reversed biosynthetic numbering is shown.

The presence of a gene coding for a dedicated first ring cyclase/dehydratase/aromatase in many aromatic polyketide gene clusters, including the PNQ gene clusters, suggests that a specific cyclase would be responsible for the aldol condensation between C-7 and C-12 (reversed biosynthetic numbering, Zhou *et al.* 2010). Recent structural and *in vitro* activity studies of a cyclase ZhuI involved in R1128 biosynthesis, homologous to PNQ cyclases, provided evidence on the dual role of ZhuI as a regiospecific first ring cyclase and a dehydratase. Initial deprotonation at position 12, which is plausible due to the weak acidity of the hydrogen next to the two carbonyl groups and resonance stabilization of the formed enolate ion, was proposed to lead to a nucleophilic attack on C-7 and subsequent protonation of the C-7 keto group. The resulting hydroxyl group was suggested to be removed via dehydration involving an enzyme catalyzed second deprotonation at position 12 and a protonation of the newly formed C-7 hydroxyl group (Fig. 5, Ames *et al.* 2011).

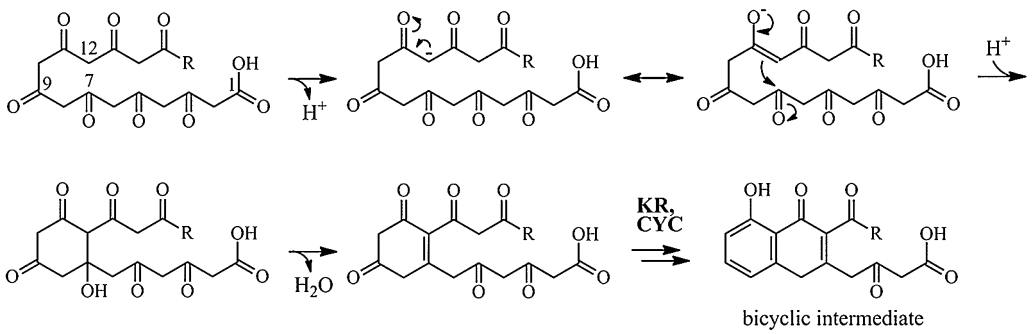

Figure 5. A model for aldol condensation and dehydration steps involved in the formation of the first aromatic ring. The C-9 keto group shown may even be reduced prior to the first ring formation. KR = C-9 ketoreductase, CYC = cyclase, R=$CH_2CH_2CH_3$ on the frenolicin pathway, and R=CH_3 on actinorhodin, granaticin and medermycin pathways.

On the actinorhodin pathway, ActIV was identified as a probable second ring cyclase responsible for another aldol condensation step. Early studies on actinorhodin biosynthesis revealed that the expression of a gene cassette coding for the actinorhodin

minimal PKS, ketoreductase ActIII, cyclase/dehydrase ActVII and second cyclase ActIV introduced into *S. coelicolor* CH999 was sufficient for the production of the three-ring naphthoquinone compounds DMAC (3,8-dihydroxy-1-methylanthraquinone-2-carboxylic acid) and its decarboxylated derivative aloesaponarin II (Fig. 4), both with the first two rings correctly cyclized (McDaniel *et al.* 1993). The presence of a gene coding for a second ring cyclase homologous to ActIV in all known PNQ gene clusters, including the partially isolated frenolicin cluster, suggests that a related cyclase of a metallo-beta-lactamase superfamily would catalyze the second ring formation on other PNQ pathways, as well.

PNQ polyketide ketoreductases and other aromatic polyketide C-9 ketoreductases are homologous NAD(P)H -dependent enzymes of the short chain dehydrogenase/reductase (SDR) family, deduced to fold into a conserved Rossmann fold. Recent structural and kinetic studies of the C-9 ketoreductase ActIII showed that the enzyme prefers bicyclic substrate analogs and is inhibited by a tricyclic compound emodin, which was bound into the active site upon cocrystallization with NADP(H) (Korman *et al.* 2008). The results support the hypothesis that C-9 ketoreduction might occur after the first ring cyclization, and that the natural substrate might even be a bicyclic pathway intermediate, but the molecular basis for the regiospecificity of the ketoreduction is still not understood very well (Korman *et al.* 2008, Javidpour *et al.* 2011). A granaticin biosynthetic enzyme of the SDR family, Gra-Orf5, was identified as a C-9 ketoreductase able to substitute for ActIII in an *in vivo* experiment (Taguchi *et al.* 2001).

2.5 The tailoring of the polyketide backbone on PNQ pathways

2.5.1 Pyran ring formation

Third ring formation can be considered the first post-PKS/tailoring step (Itoh *et al*. 2007), and it has been possible to study the biosynthetic step without the presence of minPKS enzymes. On several PNQ biosynthetic pathways, third ring formation has been suggested to involve an enzyme catalyzed ketoreduction step followed by hemiketal formation, dehydration and reduction steps, resulting in a pyran ring. On the actinorhodin pathway, ActVI-Orf1 of the 3-hydroxyacyl-CoA dehydrogenase (3HAD) protein family catalyzes the C-3 ketoreduction leading to the 3*S*-configuration of the pathway intermediate DNPA (4-dihydro-9-hydroxy-1-methyl-10-oxo-3-*H*-naphtho[2,3-*c*]pyran-3-acetic acid, Fig. 6, Ichinose *et al*. 1999, Taguchi *et al.* 2001, Taguchi *et al.* 2004). Functional studies of ActVI-Orf1 ("RED1") suggested that the enzyme would prefer non-ACP bound bicyclic substrates (Itoh *et al.* 2007). The stereospecificity of a ketoreductase Med-Orf12 from the medermycin pathway was found to be similar to its homologue ActVI-Orf1, as the

heterologous expression of *med-orf12* together with early actinorhodin biosynthetic genes resulted in the successful production of *S*-DNPA (Li *et al.* 2005).

On the granaticin pathway, the expression of *gra-orf6* in combination with early biosynthetic genes suggested that it was essential for pyran ring formation. Gra-Orf6 of the SDR protein family was thus identified as a probable C-3 ketoreductase responsible for the formation of the 3*R*-configuration in *R*-DNPA (Taguchi *et al*. 2001).

The possible C-3 ketoreduction event on the frenolicin/nanaomycin biosynthetic pathway is intriguing, but not very well understood, as the enzymes responsible for pyran ring formation are yet to be identified. The opposite stereochemistry of frenolicins and nanaomycins (Fig. 2) suggests either differentiation of the biosynthetic route and presence of alternative enzymes catalyzing this step, or relaxed stereospecificity of the biosynthetic enzymes.

On the actinorhodin pathway, ActVI-Orf2 was identified as a putative C-15 reductase responsible for completing the pyran ring synthesis and the observed (3*S*, 15*R*) configuration (Fig. 6), as inactivation of *actVI-orf2* resulted in the production of *S*-DNPA in place of actinorhodin (Fernández-Moreno *et al.* 1994). Based on amino acid (aa) sequence similarity, ActVI-Orf2 belongs to the medium-chain dehydrogenases/ reductase (MDR) family of proteins, which contain a conserved Rossmann fold domain for the binding of NAD(P)H. The biosynthetic role of the enoyl reductase ActVI-Orf2 was confirmed by recent *in vivo* experiments, as the expression of early actinorhodin biosynthetic genes in *S. coelicolor* CH999 only resulted in the successful production of dihydrokalafungin (Fig. 6) in the presence of *actVI-orf2*, while *actVI-orf1* was again found to be essential for the production of S-DNPA (Fig. 6, Fitzgerald *et al.* 2011b).

2.5.2 Tailoring stage monooxygenases

Pyran ring formation is followed by either one or two oxygenation events to complete the biosynthesis of the three-ring chromophore. The introduction of an oxygen atom into position C-6 of the central ring results in a *p*-quinone structure. Two non-related monooxygenases – ActVA-Orf6 and the two-component ActVA-Orf5–ActVB – have been shown to catalyze the same C-6 oxygenation in actinorhodin biosynthesis (Fig. 6, Kendrew *et al.* 1997, Okamoto *et al.* 2009). ActVA-Orf6 belongs to a family of cofactorless monooxygenases, and it utilizes a conserved ferredoxin fold in a dimeric fashion. The high-resolution crystal structures of the monooxygenase in complex with substrate and product analogues led to a mechanistic proposal involving the activation of molecular oxygen by the substrate 6-deoxydihydrokalafungin. An initial deprotonation of the C-13 hydroxyl group of a tautomer of the substrate was proposed to lead to the stabilization of a C-6 carbanion resonance form (Fig. 6), which could react with molecular oxygen

to form a C-6 peroxy intermediate and finally a C-6 keto group through protonation and dehydration steps (Sciara *et al.* 2003).

The ActVA-Orf5–ActVB system, on the other hand, is a two-component flavin-dependent monooxygenase, with the components belonging to acyl-CoA dehydrogenase (ACAD) and flavin reductase (FlaRed) protein families, respectively (Valton *et al.* 2006, Okamoto *et al.* 2009). The role of ActVA-Orf5–ActVB in C-8 hydroxylation, but not C-6 oxygenation, was demonstrated earlier by both *in vivo* and *in vitro* studies. The inactivation of the gene *actVB* coding for the flavin reductase component was found to result in the accumulation of the pathway intermediate kalafungin (Fig. 2), which is a γ-lactone compound oxygenated at position C-6 (Cole *et al.* 1987). Furthermore, the two-component monooxygenase was reported to catalyze the C-8 hydroxylation of a reduced hydroquinone form of dihydrokalafungin *in vitro* (Fig. 6, Valton *et al.* 2006, 2008).

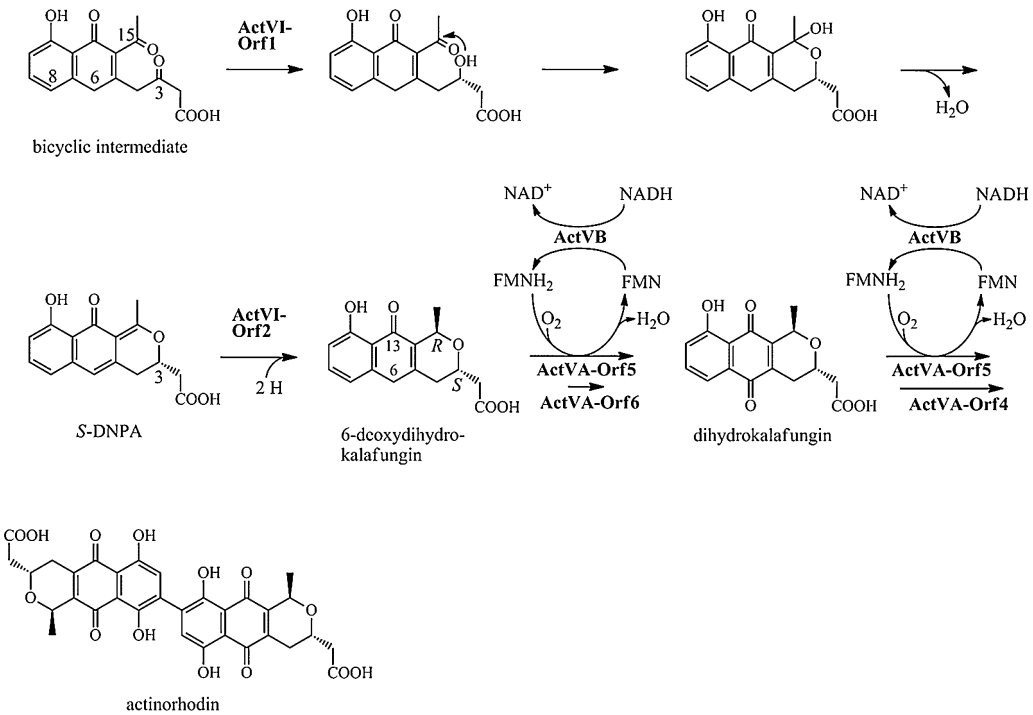

Figure 6. A simplified representation of the tailoring steps on the actinorhodin biosynthetic pathway.

The recently reported C-6 monooxygenase activity of ActVA-Orf5–ActVB was likewise confirmed both *in vitro* by the enzymatic oxygenation of a substrate analogue emodinanthrone and by *in vivo* mutagenesis studies. Co-deletion of the overlapping *actVA-orf5* and *actVA-orf6* abolished actinorhodin formation and resulted in the accumulation of actinoperylone with neither of the two positions oxygenated (Fig.

4), while the deletion of *actVA-orf6* did not seem to have any significant effect on actinorhodin production. Furthermore, the double mutant strain was complemented by the expression of *actVA-orf5*, but not *actVA-orf6*, indicating that the two-component monooxygenase was sufficient for both oxygenation events (Okamoto *et al.* 2009).

An additional oxygenation activity was recently reported for the two-component ActVA-Orf5–ActVB system (Taguchi *et al*. 2011). In accordance with earlier reports related to *in vitro* enzymatic activity of the system (Valton *et al*. 2006), C-8 oxygenation could not be observed, as the substrate dihydrokalafungin was not reduced. Instead, epoxyquinone products resembling the structure of frenolicin (Fig. 2) were obtained. The observed epoxykalafungin products were γ-lactone compounds, which could result from the oxidative lactonization of dihydrokalafungin (Taguchi *et al*. 2011). An analogous chemical oxidation of deoxyfrenolicin to a γ-lactone derivative was reported recently (Fitzgerald *et al.* 2011a).

Interestingly, both granaticin and medermycin gene clusters encode proteins homologous to the two-component ActVA-Orf5–ActVB system, but they lack a gene coding for a cofactorless monooxygenase homologous to ActVA-Orf6, although medermycin is not oxygenated at position C-8. Therefore, it is plausible that the two-component system would catalyze C-6 oxygenation on actinorhodin, granaticin and medermycin pathways (Ichinose *et al*. 2003).

Very recently, the actinorhodin monomer – 8-hydroxy-dihydrokalafungin – was isolated from an *actVA-orf4* deletion mutant strain. The gene product ActVA-Orf4 of a superfamily of Rossmann-fold NAD(P)-binding proteins was thus suggested to have a role in the dimerization of actinorhodin. However, it is not clear whether the dimerization occurs prior to or after the C-8 oxygenation (Taguchi *et al*. 2012).

2.6 The glycosylation of PNQ polyketides

Two of the PNQ polyketides discussed here are glycosylated; medermycin is decorated with an angolosamine moiety attached via a C–C bond to position C-10, while all granaticins contain a 4′-keto-2′,6′-dideoxyhexose sugar, 4′-keto- D-olivose, attached in a highly unusual manner via two C–C bonds to C-9 and C-10. In granaticin B and dihydrogranaticin B there is even a 2′,3′,6′-trideoxyhexose, L-rhodinose, attached to the first sugar via a conventional O-glycosidic bond (Fig. 2, Ichinose *et al.* 1998).

Cloning, sequencing and heterologous expression of the complete medermycin and granaticin gene clusters has enabled the identification of the probable deoxysugar biosynthetic genes (Ichinose *et al.* 1998, 2003). Sequence analysis of the medermycin gene cluster revealed six putative genes responsible for the biosynthesis of the deoxysugar

angolosamine, all of which were found next to each other and transcribed in the same direction. Many of the genes were even found to be overlapping in a manner suggestive of translational coupling (Ichinose *et al.* 2003). Sequence analysis of the granaticin cluster revealed eight gene products deduced to function in deoxysugar biosynthesis, and the genes were again found next to each other (Ichinose *et al.* 1998).

The first three biosynthetic steps are believed to be similar and catalyzed by homologous enzymes in both medermycin and granaticin deoxysugar biosynthesis. The initial formation of the activated sugar, NDP-glucose, is probably catalyzed by Med-18/ Gra-Orf16 (GraD), homologous to dTDP-glucose synthases including StrD from the biosynthetic pathway of the aminoglycoside antibiotic streptomycin (Bechthold *et al.* 1995). The next biosynthetic step is the formation of NDP-4′-keto-6′-deoxyglucose from NDP-glucose catalyzed by a dehydratase Med-17/Gra-Orf17 (GraE), again homologous to a streptomycin biosynthetic enzyme from *S. griseus*, among others (Bechthold *et al.* 1995), followed by 2′-deoxygenation catalyzed by Med-16/Gra-Orf27. On the medermycin pathway, the remaining angolosamine biosynthetic steps were suggested to be catalyzed by an aminotransferase homologue Med-20, a 4-ketoreductase Med-14 and an N-methyltransferase Med-15 (Fig. 7, Ichinose *et al.* 2003).

On the granaticin biosynthetic pathway, Gra-Orf26 was suggested to catalyze 3′-ketoreduction following the 2′-deoxygenation step catalyzed by Gra-Orf27. *In vitro* enzymatic conversion of dTDP-4′-keto-6′-deoxyglucose by Gra-Orf27 into either an unstable product or, in the presence of Gra-Orf26, a reduced 2′,6′-dideoxy product provided experimental evidence for the activities of these enzymes. Furthermore, it was proposed that the reduced 2′-deoxygenation product, dTDP-4′-keto-2′,6□-dideoxyglucose, would be transferred to the granaticin aglycone, making it the last common pathway intermediate in the biosynthesis of both the first and the second sugar of the granaticins (Fig. 7, Draeger *et al.* 1999).

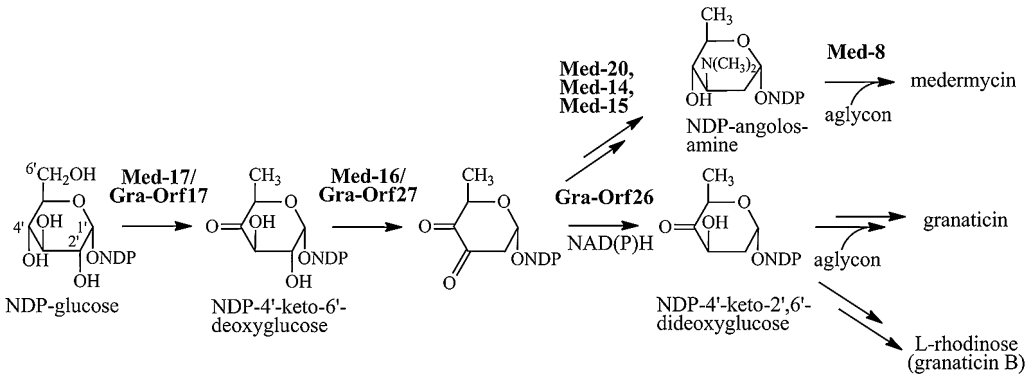

Figure 7. A simplified model for deoxysugar biosynthesis on medermycin and granaticin pathways.

Gene inactivation experiments have provided experimental evidence on the biosynthetic steps leading to the formation of the second sugar L-rhodinose in granaticin B, as individual inactivation of any of the four genes *gra-orf22–25* resulted in complete or close to complete abolishment of (dihydro)granaticin B production but did not affect the production of granaticin. Based on aa sequence similarities, Gra-Orf23 was proposed to catalyze 3′-deoxygenation, Gra-Orf25 3′(5′)-epimerization, and Gra-Orf22 4′-ketoreduction (Tornus & Floss 2001).

Only one ORF coding for a putative glycosyltransferase – *gra-orf14* – was discovered in the granaticin gene cluster. As expected, the gene product was deduced to belong to the glycosyltransferase B-family, together with most prokaryotic glycosyltransferases involved in secondary metabolite glycosylation (Thibodeaux *et al.* 2007), and to be homologous to the medermycin glycosyltransferase Med-8 (46% aa level identity). Gra-Orf14 and Med-8 are even homologous to the known C–C bond forming glycosyltransferase UrdGT2 from *Streptomyces fradiae*, which catalyzes the attachment of dTDP-D-olivose (2′,6′-dideoxy-D-glucose) in urdamycin biosynthesis (Faust *et al*. 2000). UrdGT2 was reported to also catalyze the O-glycosylation of an alternative aglycone substrate hydroxylated at a position analogous to the C-glycosylation site (Mittler *et al*. 2007).

The mechanism of C-glycosylation by UrdGT2 was suggested to resemble the mechanism described for inverting glycosyltransferases in general and to involve a general base responsible for the deprotonation of the phenolic hydroxyl group of the substrate. The nucleophilic character of the adjacent carbon would then increase through resonance, which would enable a nucleophilic attack on the activated position C-1′ of the sugar (Mittler *et al*. 2007, Härle *et al*. 2011). Interestingly, both granaticin and medermycin are C-glycosylated at an analogous *o*-position, adjacent to a hydroxylated carbon of a phenol ring (Fig. 2).

2.7 Regulatory genes in PNQ clusters

The onset of antibiotic biosynthesis in *Streptomyces* species is highly controlled and linked to growth phase, morphological stage and nutritional conditions. Antibiotic production generally occurs after the vegetative growth phase; in solid media it coincides with the onset of the formation of the aerial hyphae, while in liquid media it generally occurs at a stationary phase (Doull & Vining 1990, Bibb 1996, Hopwood 2007). The presence of an easily assimilated carbon source, such as glucose, is known to often suppress antibiotic production, although other types of nutrients may have a similar effect. Actinorhodin production in *S. coelicolor* is actively suppressed in the presence of excess glutamate as a nitrogen source as well as in the presence of excess free phosphate (Doull & Vining

1990). Additionally, N-acetyl-glucosamine has a similar effect under certain conditions (van Wezel & McDowall 2011).

Antibiotic biosynthesis and export from cells is controlled at transcriptional, translational and post-translational levels by both pleiotropic and pathway-specific regulator genes. Furthermore, the production of some transcriptional regulators controlling antibiotic biosynthesis is known to be affected by secreted hormone-like signaling compounds, of which the best known are the A-factor-like γ-butyrolactone compounds that act by binding to repressor proteins and thereby enabling the transcription of regulator genes (Bibb 1996, Hopwood 2007). The A-factor-like γ-butyrolactones are widely distributed among *Streptomyces* species, and they can control both morphological differentiation and the production of many secondary metabolites, including actinorhodin production in *S. coelicolor* (Horinouchi *et al.* 1983, Takano *et al*. 2001). The A-factor of *S. griseus* acts by binding to an A-factor receptor protein ArpA, activating the transcription of a global regulator AdpA, which – in turn – acts both as a transcriptional activator and a repressor protein by binding to certain regulatory regions. A recent study on the AdpA regulatory network in *S. griseus* revealed the complexity of the regulation; the transcription of hundreds of genes was either up- or downregulated in the absence of AdpA (Higo *et al.* 2012).

Several global, pleiotropic regulators have been reported to control actinorhodin biosynthesis is *S. coelicolor* (van Wezel & McDowall 2011). The AfsK/AfsR/AfsS system involves a protein kinase AsfK responsible for the phosphorylation of the regulator AfsR. Phosphorylated AfsR activates the transcription of a small sigma-factor like protein AfsS, which then stimulates the expression of a pathway-specific transcriptional activator ActII-Orf4. Interestingly, a phosphate response-regulator system protein PhoP was recently suggested to act as a competitive transcriptional activator of *afsS* (Santos-Beneit *et al.* 2011).

Most pathway-specific regulator proteins are transcriptional activators that act by binding to specific DNA regions upstream of the biosynthetic genes, and the activator genes have been successfully utilized in over-expression experiments resulting in increased antibiotic production (Bibb 1996). Many pathway-specific regulators belong to the family of *Streptomyces* antibiotic regulatory proteins (SARP), and the DNA-binding transcriptional activator ActII-Orf4 is one of the best characterized members of the family (Fernández-Moreno *et al*. 1991). Its gene contains a rare codon for leucine, TTA, which has a translational level regulatory role in actinorhodin production through the expression of a transfer-RNA gene *bldA* specific for the rare codon (UUA) (Bibb 1996). Gra-Orf9 and Med-Orf11 encoded by genes in granaticin and medermycin clusters, respectively, are clear homologues of ActII-Orf4 (Ichinose *et al.* 1998, 2003).

Another type of transcriptional activator gene present in PNQ clusters is *gra-orf20* coding for a putative SoxR-like activator of the MerR DNA binding superfamily. Gra-Orf20 was proposed to function by binding to certain conserved promoter sequences and activating the expression of a granaticin resistance gene in response to oxidative stress (Ichinose *et al.* 1998). Additionally, putative protein kinase regulator genes were found in granaticin and medermycin clusters (Ichinose *et al.* 2003).

Negative regulator genes were also found, as a gene (*actII-orf1*) encoding a transcriptional regulator of the tetracycline repressor (TetR) family is present in the actinorhodin cluster. Structural studies of the repressor ActII-Orf1 (ActR) in complex with either dimeric actinorhodin or two molecules of the pathway intermediate *S*-DNPA suggested that, in addition to intracellular accumulation of the end-product, even the binding of a pathway intermediate to the repressor might activate the transcription of the actinorhodin efflux pump gene *actII-orf2* (*actA*) (Willems *et al.* 2008).

2.8 Conclusions

The biosynthetic steps of type II polyketides are generally understood relatively well, and PNQ biosynthetic studies have drawn attention – the biosynthetic studies on the model compound actinorhodin in particular. Consequently, high-resolution structures of several actinorhodin biosynthetic enzymes have been obtained, most of them during the past ten years (Table 1). As already evident from the literature review above, protein structural studies have shed light on the individual functions of the enzymes, and in many cases they have been central for increased understanding of the reaction mechanisms.

Table 1. Reported structures of PNQ biosynthetic enzymes. NMR=nuclear magnetic resonance.

Name	Biosynthetic stage (description)	Method	Reference
ActI-Orf1–Orf2	minPKS (KS–CLF heterodimer)	X-ray	Keatinge-Clay *et al.* 2004
ActI-Orf3	minPKS (ACP protein)	NMR	Crump *et al.* 1997
FrnN	minPKS (ACP protein)	NMR	Li *et al.* 2003
ActIII	PKS (C-9 ketoreductase)	X-ray	Hadfield *et al.* 2004
ActVA-Orf6	tailoring (C-6 monooxygenase)	X-ray	Sciara *et al.* 2003
ActII-Orf1/ActR	regulation (repressor protein)	X-ray	Willems *et al.* 2008

Despite the success of the enzyme activity and structural studies, many important pieces of evidence are still missing. A fundamental problem is the lack of sequence information on several biosynthetic gene clusters, as complete clusters have only been cloned for actinorhodin, granaticin and medermycin (Ichinose 2003), in addition to the alnumycin gene cluster characterized in this study. Furthermore, even the complete clusters harbor genes of unknown function, which might or might not be involved in PNQ biosynthesis.

The numerous unresolved questions related to PNQ biosynthesis include the identity of the enzymes catalyzing the putative reduction and dehydration steps during frenolicin starter unit formation, the possible protein–protein interactions and the role of ACP during C-9 ketoreduction and the first ring cyclization steps, the number of common biosynthetic enzymes on frenolicin and nanaomycin pathways, and the mechanisms of the unusual C–C bond forming reactions.

3 AIMS OF THE STUDY

Initially, the main goal of the project was to identify the enzymes responsible for the formation and attachment of the unique dioxane moiety of alnumycin A and to use the gained knowledge about the biosynthetic steps in generation of novel natural products. In addition, studies related to enzymatic quinone formation on the alnumycin pathway were initiated as a side project.

Later on, the emphasis shifted towards studying the molecular basis for dioxane biosynthesis, and the main goal became to understand how the identified enzymes catalyze each biosynthetic step. Structural information on two of the biosynthetic enzymes was obtained together with collaborators, and this information was also utilized in studying the unusual reaction mechanisms.

4 MATERIALS AND METHODS

A more detailed description of the experimental procedures can be found in the original publications I–IV.

4.1 Reagents

ABTS (2,2'-Azino-bis(3-ethylbenzothiazoline-6-sulfonic acid) diammonium salt, 98%, Fluka), catalase (from bovine liver, Biochemika), glucose oxidase from *Aspergillus niger* (Fluka), NADH disodium salt hydrate (98%), NADPH tetrasodium salt (96%), peroxidase from horseradish (Fluka), D-ribose-5-phosphate disodium salt hydrate (98%) and D-ribulose-5-phosphate disodium salt (96%) were all purchased from Sigma-Aldrich. [U-^{13}C] D-ribose (98%), [5-^{13}C] D-ribose (99%) and [1-^{13}C] D-ribose (99%) were purchased from Cambridge Isotope Laboratories, Inc.

4.2 Bacterial strains and culture conditions

Alnumycin A producing *Streptomyces* sp. CM020 was obtained from Galilaeus Oy (Kaarina, Finland). *Streptomyces albus* (Chater & Wilde 1980) was used as a host strain for the heterologous expression of the gene cluster. Transformation of *S. albus* by intergeneric conjugation was conducted using *E. coli* ET12567/pUZ8002 (Kieser *et al.* 2000). Tryptone soy broth was used as a liquid medium and MS (Kieser *et al.* 2000) as a solid medium for *Streptomyces* species. For the production of secondary metabolites, *Streptomyces* strains were routinely cultivated in 25 mL of modified E1 medium (Ylihonko *et al.* 1994) with starch left out and Pharmamedia replaced by soy flour, for 5 days at 300 rpm, 301 K. Amberlite XAD 7HP (Rohm and Haas) was included for the adsorption of metabolites (1 g/50 mL). Apramycin at 50 μg/mL and thiostrepton at 50 μg/mL and 40 μg/mL were used for selection in solid and liquid media, respectively.

E. coli strains XL1-Blue MRF' (Stratagene) and TOP10 (Invitrogen) were used for cloning purposes, and the latter strain for protein production purposes. *E. coli* strains were cultivated in Luria-Bertani (LB) or 2 × tryptone yeast (TY) medium supplemented with appropriate antibiotics for the selection of plasmids and cosmids.

4.3 DNA techniques and sequence analysis

The isolation of DNA from *Streptomyces* species was performed using conventional techniques (Kieser *et al*. 2000). Restriction enzyme-digested fragments were recovered

from agarose gels using either a QIAquick or an E.Z.N.A. gel extraction kit (Qiagen or Omega Bio-Tek), whilst plasmid DNA from *E. coli* was isolated using a QIAprep Spin Miniprep Kit (Qiagen) or an E.Z.N.A. plasmid mini kit (Omega Bio-Tek). Phusion DNA Polymerase (Finnzymes) was used for polymerase chain reactions (PCRs) with 3 or 5% dimethyl sulfoxide (DMSO) to facilitate the amplification of GC-rich template sequences.

For the cloning of the alnumycin gene cluster, a genomic library of partially digested *Streptomyces* sp. CM020 DNA was constructed using a cosmid vector pFD666 and a Gigapack III XL (Stratagene) kit for packaging. After screening, one of the colonies was chosen for the sequencing of the insert DNA, which was further cloned into an *E. coli* – *Streptomyces* shuttle vector pKC505 (Kieser *et al.*. 2000) as a ca. 30-kbp fragment for heterologous expression in *Streptomyces* species. In order to enable the transformation of *Streptomyces* species by conjugation, the *aac(3)IV* region of the construct was substituted by an *aac(3)IV oriT* fragment including the *oriT* origin of replication, which was generated by PCR using pSET152 (Kieser *et al.*. 2000) as a template. The λ Red recombinase system (Datsenko & Wanner 2000) utilizing homologous recombination was used for the substitution and the resulting cosmid was named pAlnuori (I).

The ORFs *aln3*, *aln4*, *aln5*, *aln6*, *alnH* and *alnT* were individually deleted, and the overlapping ORFs *alnA* and *alnB* co-deleted from the cosmid pAlnuori using the λ Red recombinase system (Datsenko & Wanner 2000) through a two-step homologous recombination process. The primers used for inactivation consisted of a 50-nt region homologous to the target sequence followed by a 20-nt priming sequence for the amplification of the cm^R gene with flanking FRT (FLP recognition target) sites (I–III). The λ Red recombinase was utilized for the first recombination step, while the elimination of the resistance gene was executed using the helper plasmid pFLP2 expressing the FLP enzyme (Hoang *et al.* 1998).

DNA sequencing was mainly performed at Eurofins MWG Operon, Germany. The sequence analysis program Artemis (Rutherford *et al.* 2000) was used for the identification of ORFs. Comparisons to known DNA and aa sequences were performed using the Basic Local Alignment Search Tool (BLAST) of the National Center for Biotechnology Information (NCBI), USA.

4.4 Protein production and purification

For protein production purposes, individual genes were cloned into a modified pBADHisB (Invitrogen) vector (Kallio *et al.* 2006). All polyhistidine-tagged recombinant proteins carrying an N-terminal (M)AHHHHHHHRS-sequence were produced in *E. coli* TOP10 in 2 × YT medium, where L-arabinose was added to a final concentration of 0.02% (w/v,

0.006–0.01% for Aln4) at OD_{600} = 0.5–0.7 for induction. The co-expression of chaperones encoded by pG-KJE8 (Takara Bio Inc.) significantly increased the yield of His_7-Aln4 in the soluble fraction, and the induction of chaperone production was accomplished by the addition of 5 ng/mL of tetracycline into *E. coli* TOP10/pBADHisBd*aln4* cultures at an OD_{600} = 0.2–0.3. After induction, the cultures were grown at 295 K overnight, harvested at 277 K and lysed using French Press or ultra sound sonication. Triton X-100 was then routinely added to a final concentration of 0.5% (v/v).

For purification by affinity chromatography, the crude extracts were either incubated with Talon Cobalt affinity resin (Clontech), loaded onto a 1 mL HIS-select Cartridge (Sigma, AlnA) or onto a 5 mL HisTrap Ni^{2+}-affinity column (Aln4, AlnH, AlnT) as part of an ÄKTA FPLC (Fast Protein Liquid Chromatography) system (GE Healthcare), and the target proteins were eluted with increasing concentrations of imidazole. AlnH was further purified by anion exchange using a 6 mL RESOURCE Q column (GE Healthcare). The main elution fractions were subjected to buffer exchange using a PD-10 column (GE Healthcare), concentrated using a Centriprep YM-10 device (Millipore) and frozen in 50% (v/v) glycerol. Protein concentrations were typically estimated by Bradford assay (Bradford 1976).

4.5 Enzyme activity assays

Reactions were set up in a dilute buffer and ≥ 10% glycerol and premixed before alnumycin substrates were added in 2–5% DMSO to start the reactions. For all enzymes except for Aln6, the oxygen concentration was reduced using the glucose oxidase – catalase system in 60 mM D-glucose (III, IV). For specific conditions used for AlnH and AlnT, see publication II.

The incubation period of up to 3.5 h at 288 K (296 K for Aln6) was typically followed by extraction with $CHCl_3$. The $CHCl_3$ extracts were air-dried and dissolved in acetonitrile for HPLC (high-performance liquid chromatography) analysis by a SCL-10Avp system equipped with a SPD-M10Avp diode array detector (Shimadzu), and either a LiChroCART 250-4 RP-18 column (5 µm, Merck), eluted with 20 mM aqueous ammonium acetate and a 55–100% acetonitrile gradient, or a SunFire C18 column (3.5 µm, Waters) eluted with 0.1% aqueous formic acid and a 15–100% acetonitrile gradient.

Alternatively, analysis of the reaction products of AlnA was performed by separation of the acidified (2.5% HCOOH) reaction mixture on a Discovery DSC-18 column (100 mg, Supelco) in 0.1% HCOOH. The DSC-18 elution fractions in methanol were analyzed by HPLC using a Discovery HSC18 column (5 µm, 5 cm × 4.6 mm, Supelco) eluted with 20 mM aqueous ammonium acetate pH 3.6 and a 70–100% methanol gradient. Coupled AlnA and AlnB reactions with enzyme variants were followed by end-point

assays of both solvent phase samples analyzed by quantitative HPLC and water phase samples analyzed by the Malachite green method, which is based on the detection of free phosphate (Geladopoulos *et al.* 1991).

4.6 Production, purification and structural elucidation of secondary metabolites

For large scale production of secondary metabolites, the XAD 7HP resin from a total of 3 to 4 L of *Streptomyces* cultivations was separated by repeated washing with tap water and decanting. Compounds were then extracted from the resin applied on an XAD 7HP column using an aqueous acetonitrile or isopropanol gradient. Preparative scale purification of secondary metabolites typically included chloroform extractions, open column chromatography with silica gel and a final polishing step by preparative HPLC with a Merck Hitachi L-6200A (I–IV).

Structural analysis of the purified secondary metabolites and *in vitro* reaction products was accomplished using Bruker Avance NMR spectrometers, and the molecular formulae were confirmed by high resolution mass spectrometry with either ZABSpec (VG Analytical) or micrOTOF-Q (Bruker) mass spectrometers (I–IV).

5 RESULTS AND DISCUSSION

5.1 Analysis of the alnumycin gene cluster (I)

The alnumycin A producing *Streptomyces* sp. CM020 was obtained from Galilaeus Oy (Kaarina). The alnumycin gene cluster was cloned, sequenced and heterologously expressed in the *S. albus* host strain (Chater & Wilde 1980), which confirmed that a complete cluster had been isolated. Sequence analysis of the 30-kbp insert fragment enabled straightforward identification of early biosynthetic genes likely to code for starter unit and minPKS enzymes, C-9 ketoreductase and the first two cyclases, based on a relatively high aa sequence similarity to known PNQ biosynthetic gene products. Furthermore, sequence analysis enabled the preliminary identification of putative regulatory and transport proteins (Fig. 8, I).

The starter unit ketoacyl synthase gene *alnI* was found to reside separate from other early biosynthetic genes, with the last four base pairs (GTGA) overlapping with the 5′-end of a tailoring stage gene *alnH* in a manner suggestive of translational coupling. Frenolicin and R1128 starter unit ketoacyl synthases FrnI from *S. roseofulvus* (76% similarity) and ZhuH from *Streptomyces* sp. R1128 (72% similarity) are among the closest homologues of AlnI. The starter unit ACP gene *alnJ* and the acyl transferase gene *alnK* were found to reside next to each other but in opposite orientations, with the 3′-ends overlapping by 19 base pairs (Fig. 8). The highest sequence similarity to AlnJ was found for the frenolicin starter unit ACP FrnJ (73%) and, again, the starter unit ACP ZhuG from *Streptomyces* sp. R1128 was among the closest homologues. Slightly lower sequence similarity was found between the deduced starter unit acyl transferase AlnK and its homologues on frenolicin and R1128 pathways (I).

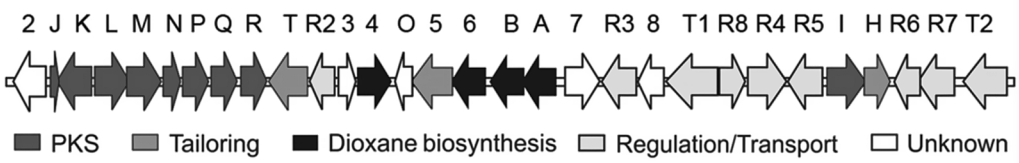

Figure 8. The organization of the alnumycin gene cluster. Deduced biosynthetic stage for each gene product is color-coded (modified from III).

In vivo cross-complementation of a benastatin starter unit synthase mutant by the co-expression of *alnI*, *alnJ* and *alnK* was reported to result in the enhanced production of butyrate-primed compounds. Thus, the combinatorial biosynthesis of benastatin derivatives verified the deduced role of the alnumycin starter unit genes in the biosynthesis of a four-carbon starter unit (Xu *et al.* 2009).

High sequence similarity to frenolicin biosynthetic enzymes – and to other PNQ biosynthetic gene products – was also found for the deduced KS AlnL, CLF AlnM, ACP AlnN, first ring cyclase AlnQ, second ring cyclase AlnR and C-9 ketoreductase AlnP. Furthermore, sequence analysis of the cloned cluster revealed that as many as seven of the thirty ORFs are likely to code for regulator proteins (Fig. 8), of which AlnR3 is a clear homologue of the SARP-family activators ActII-Orf4, Gra-Orf9 and Med-Orf11. Interestingly, *actII-orf4* and *alnR3* contain the rare codon for leucine (TTA) as the fifth or sixth codon, respectively, while *gra-orf9* and *med-orf11* do not contain TTA-codons. Thus, even AlnR3 expression is likely to be regulated at a translational level via the expression of transfer-RNA specific for the rare codon (Bibb 1996). The remaining deduced regulator genes consist of two pairs of sensory kinase/response regulator genes (*alnR4*/*alnR5* and *alnR7*/*alnR6*), and *alnR8* and *alnR2* coding for putative MarR- and TetR-family DNA-binding proteins (I).

The total number of putative regulatory genes was higher than in the closely related actinorhodin, granaticin and medermycin clusters with 2, 6 and 5 deduced regulator genes, respectively (Ichinose *et al.* 2003). However, the exact number of regulator genes in the clusters has not been confirmed, as some of the deduced regulators might not be involved in PNQ biosynthesis and, on the other hand, some genes of unknown function or not residing in the cloned fragments might have a regulatory role.

5.2 Gene products responsible for pyran ring formation (I, III)

On the basis of gene inactivation experiments, Aln4 and Aln5 were identified as gene products likely to be involved in pyran ring formation. Accumulation of the early shunt product K1115 A with an incorrectly cyclized third ring (Fig. 9) in *aln4* and *aln5* deletion mutant strains suggested that the gene products might be involved in pyran ring formation (I).

Aln4 of the aldo-keto reductase (AKR) superfamily showed the highest sequence similarity to uncharacterized proteins from *Streptomyces chartreusis* NRRL 12338 and *Sanguibacter keddieii* DSM 10542. Aln5, on the other hand, was deduced to possess a conserved lipocalin-like domain, but the exact function was not known for any of the homologous proteins. Interestingly, it showed significant sequence similarity (47%) to the C-terminal domain of a modular polyketide synthase StiJ from *Stigmatella aurantiaca*, which was proposed to catalyze chromone ring formation (Gaitatzis *et al.* 2002). Consequently, it was suggested that Aln4 might function as a C-15 ketoreductase and Aln5 as a cyclase responsible for pyran ring formation (I).

Later on, a minor secondary metabolite product of the *aln4* mutant strain was isolated from the *aln3* deletion mutant strain, and the metabolite – alnumycin B – was verified

to be a late pathway intermediate. Furthermore, Aln4 was shown to be essential for dioxane formation and to catalyze the reduction of the dioxolane unit of alnumycin B (III). Currently it remains unclear whether Aln5 alone is responsible for pyran ring formation on the alnumycin pathway.

5.3 The AlnT/AlnH monooxygenase system is essential for *p*-quinone formation (II)

Sequence analysis pointed out AlnT (413 aa) and AlnH (180 aa) as a probable two-component system responsible for quinone formation via C-8 oxygenation (reversed biosynthetic numbering) on the alnumycin pathway. AlnT belongs to an ACAD (acyl-CoA dehydrogenase) superfamily with 63% sequence similarity to ActVA-Orf5 from *S. coelicolor* A3 (2), while AlnH belongs to a FlaRed (flavin reductases) superfamily with 65% sequence similarity to ActVB from *S. coelicolor* A3 (2). As the two-component monooxygenase system ActVA-Orf5–ActVB was previously shown to catalyze both C-8 hydroxylation and C-6 oxygenation on the actinorhodin pathway (Fig. 6, Valton *et al.* 2006, Okamoto *et al.* 2009), AlnT was deduced to catalyze C-8 oxygenation. The role of the reductase component AlnH/ActVB is to provide AlnT/ActVA-Orf5 with reduced flavin, which then reacts with molecular oxygen to form a hydroperoxide intermediate utilized as an oxidant (Valton *et al.* 2006, II).

Individual inactivation of *alnH* or *alnT* resulted in strikingly similar secondary metabolite profiles. Large-scale production and purification of the metabolites revealed that, in addition to previously characterized anthraquinones K1115 A (Naruse *et al.* 1998) and DHPA (1,6-dihydroxy-8-propylanthraquinone, Huang *et al.* 2006), a novel compound named thalnumycin A was also produced (Fig. 9). K1115 A and its decarboxylated form DHPA are both oxygenated at position C-6, possibly non-enzymatically, while thalnumycin A is not oxygenated at either position C-6 or C-8 (reversed biosynthetic numbering, II). A similar lack of oxygenation was reported for actinoperylone (Fig. 4) produced by a Δ*actVA-orf5*,*6* double mutant strain (Okamoto *et al.* 2009).

The inactivation of either *actVB* or *actVA-orf5* in *S. coelicolor* was previously shown to result in the accumulation of secondary metabolites with correctly formed pyran rings (Cole *et al.* 1987, Okamoto *et al.* 2009). Surprisingly, none of the characterized metabolites of the *alnH* and *alnT* deletion mutant strains possessed a correctly formed pyran ring (Fig. 9), indicating that the oxygenation leading to quinone ring formation occurs prior to third ring formation on the alnumycin pathway, which clearly differs from the timing of these events on the actinorhodin pathway (II).

The regiospecificity of the hydroxylation was demonstrated *in vitro* through the conversion of thalnumycin A into thalnumycin B by the AlnT–AlnH system utilizing

NADH and FMN (Fig. 9). Enzymatically produced thalnumycin B was found to be relatively unstable, but it could be isolated in a sufficient quantity to enable partial structural characterization by NMR, which confirmed the *p*-hydroquinone structure of the first ring (II).

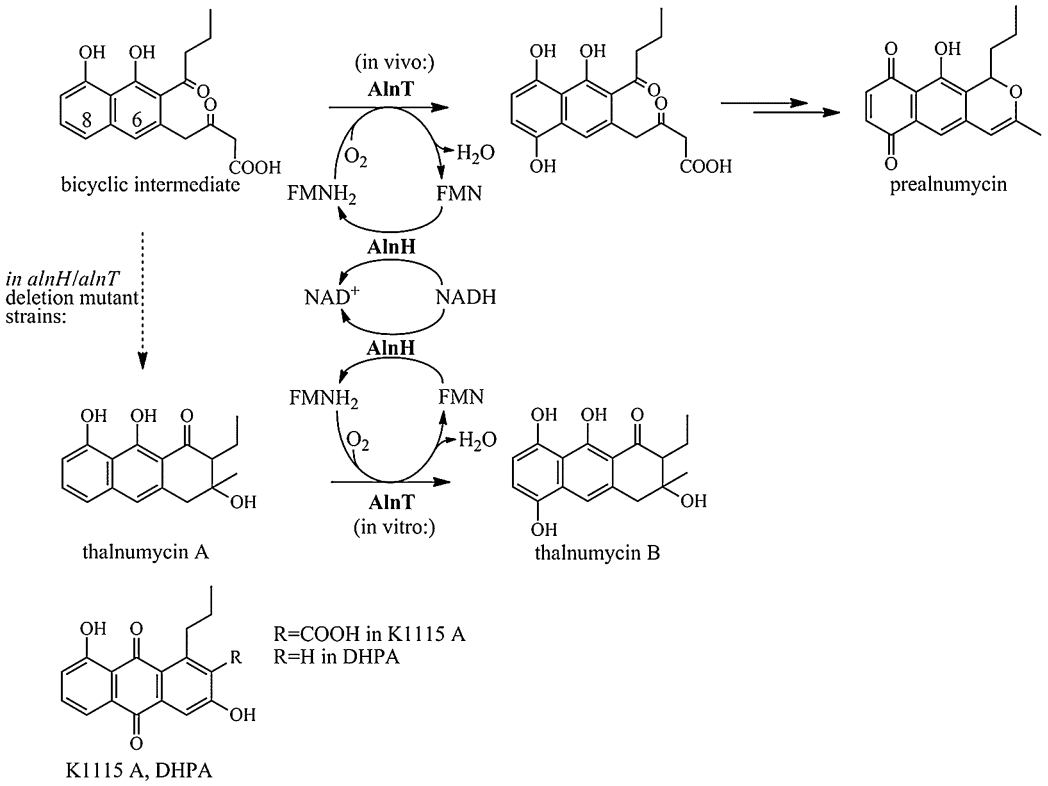

Figure 9. A model for the C-8 hydroxylation catalyzed by the two-component monooxygenase AlnT-AlnH. Structures of the secondary metabolites thalnumycin A, K1115 A and DHPA, produced by *alnH* and *alnT* deletion mutant strains, are shown.

5.4 AlnA and AlnB catalyze unusual C-ribosylation (I, III, IV)

5.4.1 Identification of the enzymes responsible for C-ribosylation (I, III, IV)

Based on sequence similarity, AlnA (306 aa) was classified as a member of the pseudouridine-5′-phosphate glycosidase protein family. Apart from AlnA, the pseudouridine-5′-phosphate glycosidases YeiN and TM1464 from *E. coli* and *Thermotoga maritima* are the only members of the protein family that have a known function, and are reported to catalyze both the hydrolysis of a glycosidic C–C bond and the reverse C–C bond formation between uracil and D-ribose-5-phosphate (Preumont *et al.* 2008). AlnB (227 aa), on the other hand,

was deduced to belong to the HAD (haloacid dehalogenase) superfamily and catalyze phosphate transfer or dephosphorylation (Allen & Dunaway-Mariano 2004).

Initial assignment of AlnA and AlnB as enzymes involved in the biosynthesis or attachment of the dioxane moiety was based on *in vivo* mutagenesis studies. Co-deletion of the overlapping ORFs from the cloned gene cluster completely abolished alnumycin A production, and the mutant strain was found to produce a novel compound, prealnumycin, lacking the dioxane unit. Expression of either gene alone could not complement the deletion (I). Later on, it was confirmed that the individual inactivation of either of the two genes resulted in a similar production profile (unpublished results).

The individual roles of the enzymes AlnA and AlnB in dioxane biosynthesis remained unknown until several pieces of experimental evidence suggested that the biosynthetic origin of the unique dioxane moiety might be D-ribose. The inactivation of an ORF *aln6* was found to result in the accumulation of alnumycin C and alnumycin D containing a ribose moiety attached to the prealnumycin aglycone, and even a single point mutation in *alnB* was found to result in the accumulation of the same compounds. The ribose moiety was found in furanose form in alnumycin C and in pyranose form in alnumycin D, and the former compound was isolated as an anomeric pair of stereoisomers only differing in the configuration of position C-1′. Of these metabolites, only the β-anomer of alnumycin C was reported earlier under the name anhydroexfoliamycin (Volkmann *et al.* 1995, III).

Furthermore, the heterologous expression construct *S. albus*/pAlnuori carrying the complete alnumycin cluster was found to produce alnumycin C and D prior to the end product during the first days of cultivation, which suggested that the compounds might be pathway intermediates (unpublished results). To study the role of D-ribose in dioxane biosynthesis, feeding experiments using 1-^{13}C-, 5-^{13}C- and universally ^{13}C-labeled D-ribose were conducted, and NMR-based analysis of the incorporation patterns of partially purified alnumycin A suggested that the complete dioxane moiety was synthesized from ribose or a closely related metabolite (III).

The role of alnumycin C as a pathway intermediate was confirmed by *in vitro* synthesis of the compound using the two enzymes AlnA and AlnB with prealnumycin and D-ribose-5-phosphate as substrates. Curiously, alnumycin D was co-produced *in vitro* only in the presence of NAD(P)H (III). At high D-ribose-5-phosphate concentrations prealnumycin appeared to be consumed even by AlnA alone, although initially no reaction products could be observed. Due to the poor solubility and stability of the compound, the AlnA reaction product was found problematic to extract, analyze and purify, but an NMR sample of sufficient quality was obtained. The product alnumycin P was verified to contain a phosphorylated ribose unit attached via a C–C bond to position C-8 of prealnumycin, and it was isolated as an anomeric pair of stereoisomers analogous to alnumycin C (IV).

After the assignment of AlnA as a C-glycosynthase catalyzing attachment of D-ribose-5-phosphate, or an alternative substrate D-ribulose-5-phosphate, the biosynthetic role of the phosphatase homologue AlnB was more straightforward to confirm. The *in vitro* dephosphorylation of purified alnumycin P to alnumycin C by AlnB alone confirmed the expected function of AlnB as a phosphatase (IV).

5.4.2 The structure of the C-glycosynthase AlnA (IV)

The 2.1-Å X-ray crystal structure of AlnA was determined by molecular replacement using the TM1464 from *T. maritima* (Levin *et al.* 2005) as a search model. AlnA was found to be folded into an α/β/α domain involving a twisted, nine-stranded mixed β-sheet surrounded be three α-helices on one side and four α-helices on the other side. Two additional β-strands, a metal ion and a small lid-like helix-turn-helix motif were observed on top of the β-sheet. A structural similarity search revealed that AlnA is significantly similar in structure only to the pseudouridine-5′-phosphate glycosidase TM1464, and both proteins were found to crystallize in a trimeric form (Levin *et al.* 2005, IV).

A 3.15-Å structure of a complex with a phosphorylated sugar bound to the putative active site was obtained by soaking AlnA crystals in 100 mM D-ribose-5-phosphate. The electron density for the observed ligand was found to best fit to D-ribulose-5-phosphate, which is an alternative substrate for AlnA, or a linear aldehyde form of D-ribose-5-phosphate. The binding of the linear D-ribulose-5-phosphate by AlnA was also confirmed using NMR based methods. The phosphate moiety was found to be coordinated to His130, Ser140 and to the metal ion, which is most likely Ca^{2+} (IV). Interestingly, a relatively similar unidentified ligand, larger than glycerol-3-phosphate, was observed in the 1.9-Å crystal structure of TM1464 (Levin *et al.* 2005).

5.4.3 The structure of the phosphatase AlnB (IV)

The 1.25-Å crystal structure of AlnB was determined by molecular replacement using the core domain of a putative phosphatase from *Haemophilus somnus* as a search model. AlnB was found to consist of a modified Rossmann fold domain similar to the core domain of other members of the HAD family, and of a four-helix bundle cap domain. Based on the structure of the cap domain, AlnB could be classified as a member of subfamily I (Allen & Dunaway-Mariano 2004). A metal ion, most likely Mg^{2+}, was observed in the junction between the core and cap domains, and the residues Asp15, Asp175 and the backbone carbonyl oxygen of Asp17 were found to be involved in the coordination of the metal ion (IV).

In HAD family proteins, the catalytic platform is created by core domain residues, while the cap domain is considered important for substrate recognition. On the

other hand, the lack of a cap domain, which is observed for enzymes of subfamily III, enables the binding of larger substrates (Allen & Dunaway-Mariano 2004). The substrate of AlnB, alnumycin P (Fig. 10), is relatively large for a subfamily I enzyme but could be modeled inside a narrow cavity within the four-helix bundle, with the phosphate moiety next to the metal ion, as observed in the complex with free phosphate (IV).

5.4.4 Proposed mechanism for C-ribosylation (III, IV)

AlnA was found to catalyze the slow interconversion of D-ribose-5-phosphate and D-ribulose-5-phosphate in solution, which occurs via a linear ene-diol species (IV). This finding, together with the observed linear phosphosugar in the complex structure of AlnA, and the ability of both D-ribose-5-phosphate and D-ribulose-5-phosphate to serve as substrates for AlnA (III), provided strong evidence for a mechanistic proposal involving a linear phosphosugar species as a substrate for the C-ribosylation of prealnumycin (Fig. 10, IV).

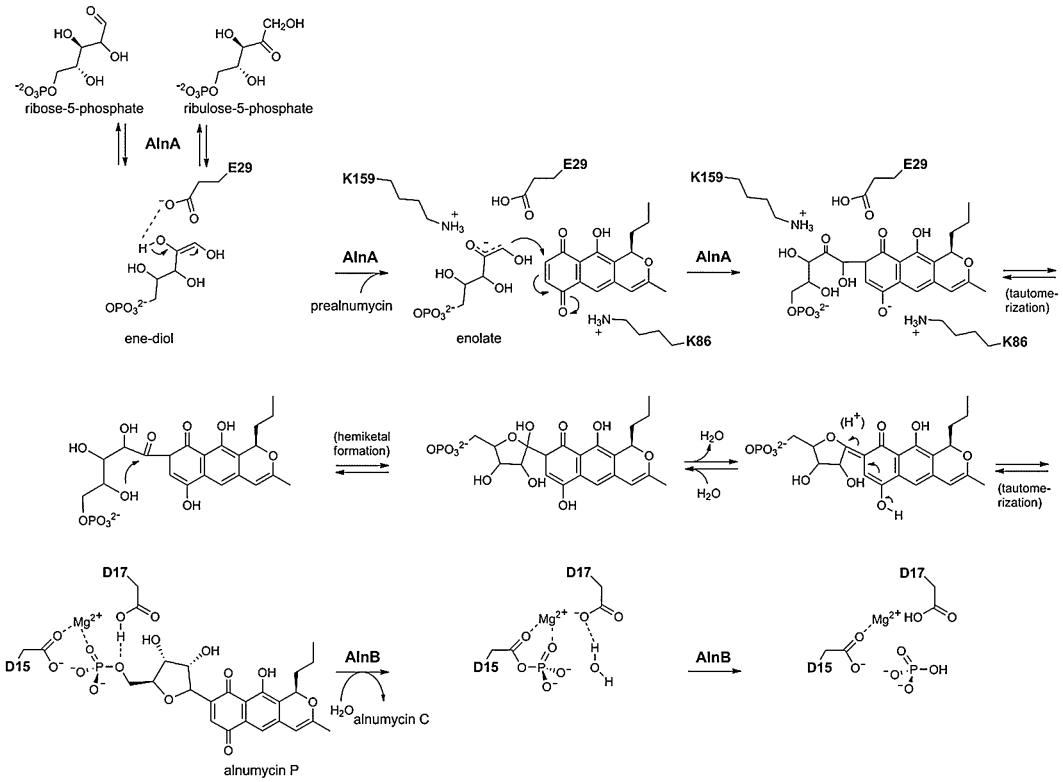

Figure 10. Proposed mechanism for C-ribosylation of prealnumycin by AlnA and AlnB. Selected active site residues of AlnA (upper part) and AlnB (lower part) are shown in bold (modified from IV).

In the initial step, Glu29 is suggested to act as a general base and abstract a proton of a hydroxyl group at position C-2′ of the ene-diol intermediate. The observed distance (4.3 Å) between Glu29 and the probable C-2′ oxygen in the AlnA complex structure might be small enough to support this catalytic role for Glu29. The formed enolate anion would be resonance-stabilized and able to act as a nucleophile attacking the position C-8 of prealnumycin in a manner characteristic of a Michael-type addition mechanism to an α,β-unsaturated carbonyl compound. The intermediate anion formed at this step could be stabilized by ionic interaction with Lys86 or protonated. Cyclization of the attached sugar might then occur even non-enzymatically, resulting in the formation of alnumycin P (IV). Condition-dependent formation of alnumycin D by AlnA and AlnB *in vitro* (III) supports the proposed model for spontaneous cyclization, although in the case of alnumycin D dephosphorylation of the open-chain intermediate (Fig. 10) should occur prior to cyclization.

A Michael-type 1,4-addition mechanism was supported by the mutagenesis of AlnA active site residues. The enzymatic activity assays with AlnA variants were performed as coupled end-point assays, and they revealed close to complete inactivation of AlnA by the mutagenesis of Glu29 to Gln. In addition, the activities of the alanine variants of Glu29, Lys159 and Lys86 were found to be relatively low (IV).

In general, the mechanism proposed for AlnA does not resemble the mechanisms described for known prokaryotic glycosyltransferases, which involve a nucleophilic attack on the activated position of an NDP-sugar (Thibodeaux *et al*. 2007, Chang *et al*. 2011). In contrast, it is the sugar species that acts as a nucleophile in the proposed C-ribosylation mechanism (Fig. 10, IV).

Dephosphorylation of alnumycin P to alnumycin C by the phosphatase AlnB was suggested to involve the putative catalytic residues Asp15 and Asp17, which was supported by the mutagenesis of these residues. The relative activity of AlnB variants was measured in a coupled assay with AlnA, and the individual mutagenesis of the conserved Asp15 and Asp17 to alanine residues was found to result in close to inactive AlnB. Asp17 is likely to act as a general acid/base, which protonates the leaving group – in this case the C-5′ oxygen of alnumycin P. Asp15, in turn, is likely to be responsible for a nucleophilic attack on the phosphorus. In the next step, Asp17 may act as a general base and aid in the generation of a final nucleophile from water. The mutagenesis of Lys119 to an alanine or arginine residue reduced the enzyme activity to only about 4% vs. 2%. Based on modeling results, the finding may be due to an effect on the binding of the substrate (IV). In general, the mutagenesis results were well in line with other phosphatases of the HAD family (Allen & Dunaway-Mariano 2004).

5.5 Aln6 is a novel riboisomerase (III)

5.5.1 The function of Aln6 (III)

Inactivation of the ORF *aln6* was essential for the identification of Aln6 (359 aa) as a dioxane biosynthetic enzyme, as functions are not known for any of the homologous proteins. Interestingly, these include ActVA-3 from *S. coelicolor* A3 (2), Gra-Orf28 and Gra-Orf30 from *S. violaceoruber*, as well as Aln7 from the alnumycin gene cluster. Aln6 was found to be essential for dioxane biosynthesis, as deletion of the *aln6* gene abolished the production of alnumycin A, and the mutant strain *S. albus*/pAlnuoriΔ*aln6* accumulated novel C-ribosylated compounds alnumycin C and alnumycin D (III, see section 5.4.1).

The *in vitro* enzymatic conversion of alnumycin C to alnumycin B carrying a dioxolane unit in place of a ribose unit confirmed the biosynthetic role of Aln6. Alnumycin D, on the other hand, could not be converted by Aln6. Unexpectedly, no apparent cofactors were necessary for the oxidative conversion, although Aln6 was found to consume molecular oxygen and produce hydrogen peroxide during the conversion of alnumycin C (Fig. 11). Based on these findings, Aln6 could be classified as a novel riboisomerase or a novel cofactorless oxidase (III).

5.5.2 Proposed mechanism for dioxolane formation (III)

The oxidative conversion of the ribose unit in alnumycin C into the dioxolane unit of alnumycin B involves cleavage of a C–C bond. The cleavage site was confirmed by feeding experiments with labeled D-ribose species; 1-^{13}C- and 5-^{13}C-carbons of ribose were specifically incorporated into positions C-1′ and C-5′ of alnumycin B (Fig. 11, III).

The labeling experiments, together with the stoichiometric consumption of molecular oxygen, detected production of hydrogen peroxide and the changes observed in the UV-Vis spectrum of the alnumycins enabled a mechanistic proposal for dioxolane formation. In the initial step, deprotonation at position C-1′ was suggested to lead to the formation of a highly conjugated intermediate with a UV-Vis spectrum likely to differ from the distinctive alnumycin spectrum. The intermediate anion could then react with oxygen to form a hydroperoxy intermediate. Loss of hydrogen peroxide would generate a double bond between C-1′ and C-2′, and a following hydration step would yield a hydroxylated intermediate. Up to this stage, the mechanism would be similar to the well-characterized hydroxylation mechanism of urate oxidase, which is a cofactorless oxidase (Gabison *et al.* 2008). Subsequent ring opening and tautomerization steps would enable an aldol cleavage of the C-1′–C-2′ bond. The dioxolane unit could then be formed through hemiacetal and acetal formation steps (Fig. 11, III).

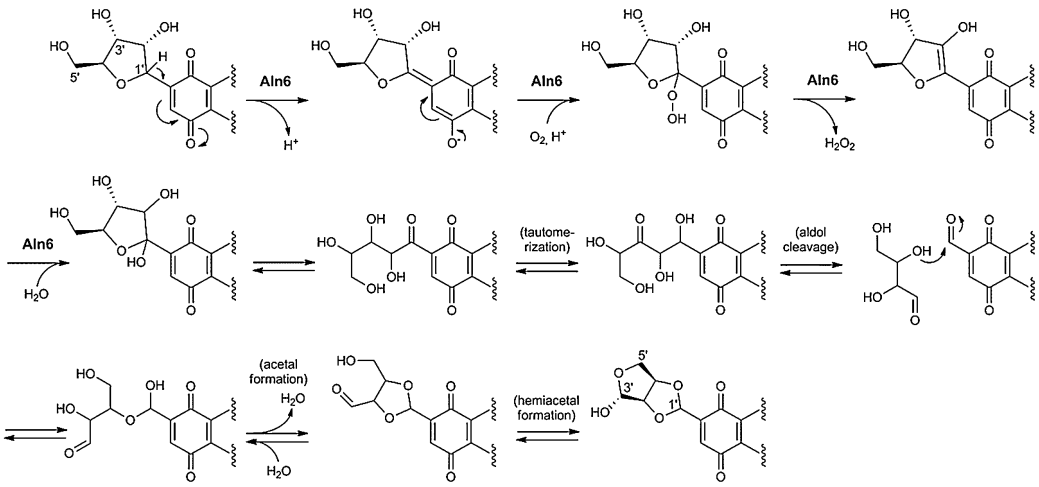

Figure 11. Proposed mechanism for dioxolane formation by Aln6. Only the quinone ring of the prealnumycin moiety is shown. Carbon numbering is given for the ribose unit in the substrate alnumycin C and for the dioxolane unit in the product alnumycin B (modified from III).

5.6 The reductase Aln4 catalyzes the conversion of dioxolane to dioxane (I, III)

Aln4 (354 aa) belongs to a family of NAD(P)H-dependent aldo-keto reductases (AKRs) deduced to catalyze a reduction of an aldehyde or ketone to an alcohol. Initially, Aln4 was assigned as a C-15 ketoreductase involved in pyran ring formation, based on the secondary metabolite profile of the *aln4* mutant strain; inactivation of *aln4* resulted in complete abolishment of alnumycin A production, and accumulation of the shunt product K1115 A together with relatively low levels of an unknown side product (I). The minor metabolite, alnumycin B, was later characterized and found to consist of a highly unusual dioxolane (*cis*-bicyclo[3.3.0]-2′,4′,6′-trioxaoctan-3′β-ol) moiety attached via a C-1′–C-8 bond to the prealnumycin aglycone (Fig. 11). In a manner analogous to alnumycin P and alnumycin C, the compound was again isolated as an epimeric pair of stereoisomers only differing at position C-1′ (III).

The ORF *aln4* was found to be separated by only 3 bp from the upstream ORF *aln3*. Curiously, the *aln3* mutant strain was found to only produce low levels of alnumycin A, and alnumycin B as its main secondary metabolite. The relatively high levels of alnumycin B produced suggested that *aln3* might be involved in a late biosynthetic step, but no additional evidence supporting a possible biosynthetic role for *aln3* was obtained (III).

The enzymatic *in vitro* conversion of alnumycin B to alnumycin A by Aln4 confirmed the biosynthetic role of Aln4 as an NADPH-dependent reductase catalyzing the conversion

of a dioxolane unit into the dioxane unit of alnumycin A. Additionally, a novel *in vitro* side product, alnumycin S, was isolated and found to contain the dioxolane moiety reduced at position C-3′ (numbering for alnumycin B). Aln4 was thus verified to catalyze the reduction of the open-ring aldehyde form of alnumycin B to an alcohol (Fig. 12, III).

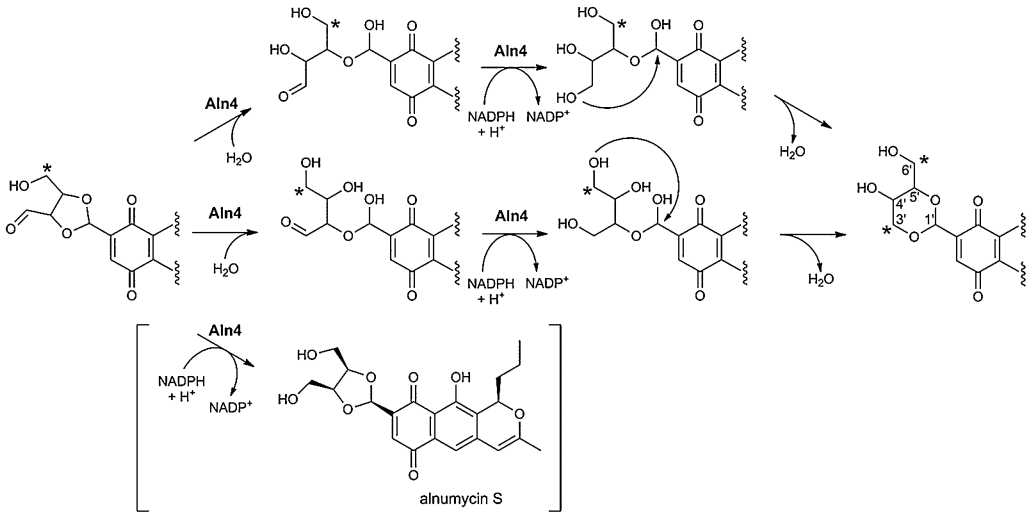

Figure 12. A model for dioxane formation by Aln4. The formation of the *in vitro* side product alnumycin S is shown in brackets. The incorporation of the 5-^{13}C D-ribose label into the dioxolane unit of alnumycin B and the dioxane unit of alnumycin A is marked with asterisks (modified from III).

An additional ring opening is necessary for the formation of the 6-membered dioxane ring from dioxolane. As alnumycin S could not be converted further by Aln4, it is plausible that the ring opening needs to take place prior to the reduction step. The ring opening would putatively occur through the hydration of the acetal, resulting in two alternative aldehyde products, which could then be reduced by Aln4. A final acetal formation step would result in a dioxane product. The mechanistic proposal was supported by feeding experiment results, which revealed that the 5-^{13}C-label of D-ribose was incorporated into two alternative positions in the end product alnumycin A (Fig. 12, III).

The recent characterization of the stereoisomers of the end product alnumycin A (Oja *et al*. 2012, Tähtinen *et al*. 2012, see section 2.2) is in line with the proposed mechanism for Aln4. Although the suggested mechanism does not require any configurational changes at positions C-4′ or C-5′ (numbering for alnumycin A), these might occur e.g. via the tautomerization of an open-chain aldehyde intermediate (Fig. 12). However, more detailed biosynthetic and mechanistic studies would be necessary to confirm the biosynthetic origin of the stereoisomers of alnumycin A.

6 CONCLUDING REMARKS

The experimental evidence obtained during the thesis project has significantly contributed to the understanding of alnumycin biosynthesis, in particular to the understanding of the dioxane biosynthetic steps. The main results include functional analysis of the two-component monooxygenase AlnH–AlnT, which is responsible for the enzymatic oxygenation of the polyketide aglycone, and characterization of the dioxane biosynthetic pathway involving the enzymes AlnA, AlnB, Aln6 and Aln4 (Fig. 13).

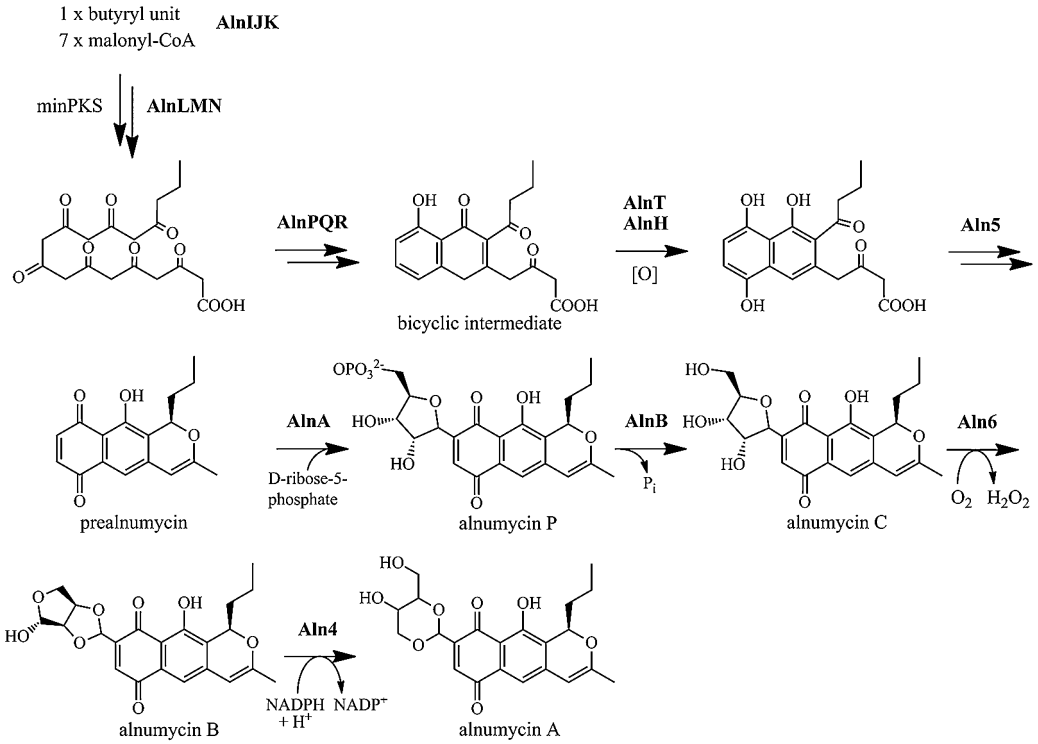

Figure 13. A model for the alnumycin biosynthetic pathway. For simplicity, the stereoisomers of alnumycins A, B, C and P are not shown.

Most of the enzymes responsible for dioxane biosynthesis were found to catalyze unusual reactions or to utilize uncommon reaction mechanisms. In fact, there are no previous mechanistic level studies related to the rare C-ribosylation catalyzed by AlnA. The apparently cofactorless enzyme Aln6, in turn, was found to convert the ribose unit of the pathway intermediate alnumycin C into the rare dioxolane unit of the next pathway intermediate, alnumycin B, via a mechanism that involves the consumption of molecular oxygen coupled to the formation of hydrogen peroxide. Finally, the deduced aldo-keto reductase Aln4 was found to catalyze not only the reduction of an aldehyde to an alcohol,

but also the reductive conversion of the dioxolane unit to the dioxane unit of the pathway end product alnumycin A (Fig. 13).

Characterization of the novel dioxane pathway illustrates how unique sugar mimicking units can be made from simple sugar-5-phosphate precursors, and the knowledge gained on the biosynthetic steps and enzymes might be applicable for drug discovery purposes. The usefulness of the dioxane biosynthetic enzymes in the generation of novel compounds with C–C bound ribose, dioxolane and dioxane moieties is currently under investigation in a follow-up study in our laboratory. In addition, a collaborative study on the biological activities of the novel natural products, that were isolated and characterized during the thesis work, has been initiated.

ACKNOWLEDGEMENTS

Most of the experimental work related to this thesis was carried out during the years 2006–2012 in the Antibiotic Biosynthetic Enzymes (ABE) research group at the Department of Biochemistry and Food Chemistry, University of Turku. The National Doctoral Programme in Informational and Structural Biology (ISB) is acknowledged for providing important long-term funding and other support for the thesis project, and the Academy of Finland for additional funding, which enabled the completion of the project.

I had the privilege to become a member of the former *Streptomyces* research group already in 2003, and I'm grateful to Kaisa Palmu for teaching me all the basics about working with the fascinating *Streptomyces* species. A big and warm thank you to all the supervisors of my doctoral thesis: Jarmo Niemi, Pekka Mäntsälä and Mikko Metsä-Ketelä in particular. You gave me the chance to choose an interesting and challenging project, and – importantly – did not leave me alone with the project. Furthermore, I wish to thank Prof. Reijo Lahti and my Thesis Committee Member, Adjunct Prof. Tiina Salminen for advice and encouragement. I also want to thank our collaborators Prof. Gunther Schneider from Karolinska Institutet, Stockholm, and Dr. Karel Klika from the Department of Chemistry for pleasant collaboration and insightful comments on the work.

It has been both fun and inspiring to work in Arcanum, and I wish to acknowledge Prof. Heino for the excellent facilities and all the Biochemistry staff for the great atmosphere, which has made this a pleasant period altogether. A special thanks for all the good times to both former and current members of the team: Pauli, Thadee, Pekka, Bastian, Vilja, Laila and all the others (sorry for not being able to list all the names here).

Finally, I want to thank our close, dear relatives for their support and help, which really mean a lot to me. And – of course – my deepest gratitude belongs to Petri, Arttu and Aliisa for all the support, joy and love.

REFERENCES

Allen K.N., Dunaway-Mariano D. **(2004)** Phosphoryl group transfer: evolution of a catalytic scaffold. *Trends Biochem. Sci.* **29**, 495–503.

Ames B.D., Lee M.-Y., Moody C., Zhang W., Tang Y., Tsai S.-C. **(2011)** Structural and biochemical characterization of ZhuI aromatase/cyclase from the R1128 polyketide pathway. *Biochemistry* **50**, 8392–8406.

Arthur C.J., Szafranska A., Evans S.E., Findlow S.C., Burston S.G., Owen P., Clark-Lewis I., Simpson T.J., Crosby J., Crump M.P. **(2005)** Self-malonylation is an intrinsic property of a chemically synthesized type II polyketide synthase acyl carrier protein. *Biochemistry* **44**, 15414–15421.

Bechthold A., Sohng J.K., Smith T.M., Chu X., Floss H.G. **(1995)** Identification of *Streptomyces violaceoruber* Tü22 genes involved in the biosynthesis of granaticin. *Mol. Gen. Genet.* **248**, 610–620.

Bérdy J. **(2012)** Thoughts and facts about antibiotics: Where we are now and where we are heading. *J. Antibiot. (Tokyo)* **65**, 385–395.

Bibb M. **(1996)** 1995 Colworth Prize Lecture. The regulation of antibiotic production in *Streptomyces coelicolor* A3(2). *Microbiology* **142**, 1335–1344.

Bibb M.J., Sherman D.H., Omura S., Hopwood D.A. **(1994)** Cloning, sequencing and deduced functions of a cluster of *Streptomyces* genes probably encoding biosynthesis of the polyketide antibiotic frenolicin. *Gene* **142**, 31–39.

Bieber B., Nüske J., Ritzau M., Gräfe U. **(1998)** Alnumycin a new naphthoquinone antibiotic produced by an endophytic *Streptomyces* sp. *J. Antibiot. (Tokyo)* **51**, 381–382.

Björn B., Jörg N. **(1998)** Alnumycin useful as antibiotic. Patent number: DE19745914.

Bradford M.M. **(1976)** A rapid and sensitive method for the quantitation of microgram quantities of protein utilizing the principle of protein-dye binding. *Anal. Biochem.* **72**, 248–254.

Brimble M.A., Duncalf L.J., Nairn M.R. **(1999)** Pyranonaphthoquinone antibiotics--isolation, structure and biological activity. *Nat. Prod. Rep.* **16**, 267–281.

Brünker P., McKinney K., Sterner O., Minas W., Bailey J.E. **(1999)** Isolation and characterization of the naphthocyclinone gene cluster from *Streptomyces arenae* DSM 40737 and heterologous expression of the polyketide synthase genes. *Gene* **227**, 125–135.

Carreras C.W., Khosla C. **(1998)** Purification and in vitro reconstitution of the essential protein components of an aromatic polyketide synthase. *Biochemistry* **37**, 2084–2088.

Chang A., Singh S., Phillips G.N.Jr., Thorson J.S. **(2011)** Glycosyltransferase structural biology and its role in the design of catalysts for glycosylation. *Curr. Opin. Biotechnol.* **22**, 800–808.

Chater K.F., Wilde L.C. **(1980)** *Streptomyces albus* G mutants defective in the *Sal*GI restriction-modification system. *J. Gen. Microbiol*. **116**, 323–334.

Cole S.P., Rudd B.A., Hopwood D.A., Chang C.J., Floss H.G. **(1987)** Biosynthesis of the antibiotic actinorhodin. Analysis of blocked mutants of *Streptomyces coelicolor*. *J. Antibiot. (Tokyo)* **40**, 340–347.

Cox R.J., Crosby J., Daltrop O., Glod F., Jarzabek M.E., Nicholson T.P., Reed M., Simpson T.J., Smith L.H., Soulas F., Szafranska A.E., Westcott J. **(2002)** *Streptomyces coelicolor* phosphopantetheinyl transferase: a promiscuous activator of polyketide and fatty acid synthase acyl carrier proteins. *J. Chem. Soc., Perkin Trans. 1*, 1644–1649.

Crump M.P., Crosby J., Dempsey C.E., Parkinson J.A., Murray M., Hopwood D.A., Simpson T.J. **(1997)** Solution structure of the actinorhodin polyketide synthase acyl carrier protein from *Streptomyces coelicolor* A3(2). *Biochemistry* **36**, 6000–6008.

Dall'Aglio P., Arthur C. J., Williams C., Vasilakis K., Maple H. J., Crosby J., Crump M. P., Hadfield A.T. **(2011)** Analysis of *Streptomyces coelicolor* Phosphopantetheinyl Transferase, AcpS, Reveals the Basis for Relaxed Substrate Specificity. *Biochemistry* **50**, 5704–5717.

Datsenko K.A., Wanner B.L. **(2000)** One-step inactivation of chromosomal genes in *Escherichia coli* K-12 using PCR products. *Proc. Natl. Acad. Sci. U. S. A.* **97**, 6640–6645.

Doull J.L., Vining L.C. **(1990)** Nutritional control of actinorhodin production by *Streptomyces coelicolor* A3(2): suppressive effects of nitrogen and phosphate. *Appl. Microbiol. Biotechnol.* **32**, 449–454.

Draeger G., Park S.-H., Floss H.G. **(1999)** Mechanism of the 2-Deoxygenation Step in the Biosynthesis of the Deoxyhexose Moieties of the Antibiotics Granaticin and Oleandomycin. *J. Am. Chem. Soc.* **121**, 2611–2612.

Dreier J., Khosla C. **(2000)** Mechanistic analysis of a type II polyketide synthase. Role of conserved residues in the beta-ketoacyl synthase-chain length factor heterodimer. *Biochemistry* **39**, 2088–2095.

Ellestad G.A., Kunstmann M.P., Whaley H.A., Patterson E.L. **(1968)** The structure of frenolicin. *J. Am. Chem. Soc.* **90**, 1325–1332.

Evans S.E., Williams C., Arthur C.J., Płoskoń E., Wattana-amorn P., Cox R.J., Crosby J., Willis C.L., Simpson T.J., Crump M.P. **(2009)** Probing the Interactions of early polyketide intermediates with the Actinorhodin ACP from *S. coelicolor* A3(2). *J. Mol. Biol.* **389**, 511–528.

Faust B., Hoffmeister D., Weitnauer G., Westrich L., Haag S., Schneider P., Decker H., Künzel E., Rohr J., Bechthold A. (**2000)** Two new tailoring enzymes, a glycosyltransferase and an oxygenase, involved in biosynthesis of the angucycline antibiotic urdamycin A in *Streptomyces fradiae* Tü2717. *Microbiology* **146**, 147–154.

Fernández-Moreno M.A., Caballero J., Hopwood D.A., Malpartida F. **(1991)** The *act* cluster contains regulatory and antibiotic export genes, direct targets for translational control by the *bldA* tRNA gene of streptomyces. *Cell* **66**, 769–780.

Fernández-Moreno M.A., Martínez E., Caballero J.L., Ichinose K., Hopwood D.A., Malpartida F. **(1994)** DNA sequence and functions of the *act*VI region of the actinorhodin biosynthetic gene cluster of *Streptomyces coelicolor* A3(2). *J. Biol. Chem.* **269**, 24854–24863.

Fitzgerald J.T., Henrich P.P., O'Brien C., Krause M., Ekland E.H., Mattheis C., Sa J.M., Fidock D., Khosla C. **(2011a)** *In vitro* and *in vivo* activity of frenolicin B against *Plasmodium falciparum* and *P berghei*. *J. Antibiot. (Tokyo)* **64**, 799–801.

Fitzgerald J.T., Ridley C.P., Khosla C. **(2011b)** Engineered biosynthesis of the antiparasitic agent frenolicin B and rationally designed analogs in a heterologous host. *J. Antibiot. (Tokyo)* **64**, 759–762.

Gabison L., Prangé T., Colloc'h N., El Hajji M., Castro B., Chiadmi M. **(2008)** Structural analysis of urate oxidase in complex with its natural substrate inhibited by cyanide: mechanistic implications. *BMC Struct. Biol.* **8**, 32.

Gago G., Diacovich L., Arabolaza A., Tsai S.C., Gramajo H. **(2011)** Fatty acid biosynthesis in actinomycetes. *FEMS Microbiol. Rev.* **35**, 475–497.

Gaitatzis N., Silakowski B., Kunze B., Nordsiek G., Blöcker H., Höfle G., Müller R. **(2002)** The biosynthesis of the aromatic myxobacterial electron transport inhibitor stigmatellin is directed by a novel type of modular polyketide synthase. *J. Biol. Chem.* **277**, 13082–13090.

Geladopoulos T.P., Sotiroudis T.G., Evangelopoulos A.E. **(1991)** A malachite green colorimetric assay for protein phosphatase activity. *Anal. Biochem.* **192**, 112–116.

Gibson-Clay G., Byrn S.R., Heinstein P. **(1982)** The interaction of granaticin with nucleic acids and pyruvate decarboxylase. *J. Pharm. Sci.* **71**, 467–468.

Gross F., Luniak N., Perlova O., Gaitatzis N., Jenke-Kodama H., Gerth K., Gottschalk D., Dittmann E., Müller R. **(2006)** Bacterial type III polyketide synthases: phylogenetic analysis and potential for the production of novel secondary metabolites by heterologous expression in pseudomonads. *Arch. Microbiol.* **185**, 28–38.

Hadfield A.T., Limpkin C., Teartasin W., Simpson T.J., Crosby J., Crump M.P. **(2004)** The Crystal Structure of the actIII Actinorhodin Polyketide Reductase: Proposed Mechanism for ACP and Polyketide Binding. *Structure* **12**, 1865–1875.

Heinstein P. **(1982)** Mechanism of action of granaticin: inhibition of ribosomal RNA maturation and cell cycle specificity. *J. Pharm. Sci.* **71**, 197–200.

Higo A., Hara H., Horinouchi S., Ohnishi Y. **(2012)** Genome-wide distribution of AdpA, a global regulator for secondary metabolism and morphological differentiation in Streptomyces, revealed the extent and complexity of the AdpA regulatory network. *DNA Res*. **19**, 259–274.

Hitchman T.S., Crosby J., Byrom K.J., Cox R.J., Simpson T.J. (**1998**) Catalytic self-acylation of type II polyketide synthase acyl carrier proteins. *Chem. Biol*. **5**, 35–47.

Hoang T.T., Karkhoff-Schweizer R.R., Kutchma A.J., Schweizer H.P. **(1998)** A broad-host-range Flp-FRT recombination system for site-specific excision of chromosomally-located DNA sequences: application for isolation of unmarked *Pseudomonas aeruginosa* mutants. *Gene* **212**, 77–86.

Hopwood D.A. **(2007)** Streptomyces in Nature and Medicine: The Antibiotic Makers. Oxford University Press, USA.

Horinouchi S., Hara O., Beppu T. **(1983)** Cloning of a pleiotropic gene that positively controls biosynthesis of A-factor, actinorhodin, and prodigiosin in *Streptomyces coelicolor* A3(2) and *Streptomyces lividans*. *J. Bacteriol.* **155**, 1238–1248.

Huang Y.F., Tian L., Sun Y., Pei Y.H. **(2006)** Two new compounds from marine *Streptomyces* sp. FX-58. *J. Asian Nat. Prod. Res*. **8**, 495–498.

Huffman J., Gerber R., Du L. **(2010)** Recent advancements in the biosynthetic mechanisms for polyketide-derived mycotoxins. *Biopolymers* **93**, 764–776.

Hultin P.G. **(2005)** Bioactive C-Glycosides from Bacterial Secondary Metabolism. *Curr. Top. Med. Chem.* **5**, 1299–1331.

Härle J., Günther S., Lauinger B., Weber M., Kammerer B., Zechel D.L., Luzhetskyy A., Bechthold A. **(2011)** Rational design of an aryl-C-glycoside catalyst from a natural product O-glycosyltransferase. *Chem. Biol.* **18**, 520–530.

Ichinose K., Bedford D.J., Tornus D., Bechthold A., Bibb M.J., Revill W.P., Floss H.G., Hopwood D.A. **(1998)** The granaticin biosynthetic gene cluster of *Streptomyces violaceoruber* Tü22: sequence analysis and expression in a heterologous host. *Chem. Biol.* **5**, 647–659.

Ichinose K., Surti C., Taguchi T., Malpartida F., Booker-Milburn K.I., Stephenson G.R., Ebizuka Y., Hopwood D.A. **(1999)** Proof that the *act*VI genetic region of *Streptomyces coelicolor* A3(2) is involved in stereospecific pyran ring formation in the biosynthesis of actinorhodin. *Bioorg. Med. Chem. Lett.* **9**, 395–400.

Ichinose K., Ozawa M., Itou K., Kunieda K., Ebizuka Y. **(2003)** Cloning, sequencing and heterologous expression of the medermycin biosynthetic gene cluster of *Streptomyces* sp. AM-7161: towards comparative analysis of the benzoisochromanequinone gene clusters. *Microbiology* **149**, 1633–1645.

Itoh T., Taguchi T., Kimberley M.R., Booker-Milburn K.I., Stephenson G.R., Ebizuka Y., Ichinose K. **(2007)** Actinorhodin biosynthesis: structural requirements for post-PKS tailoring intermediates revealed by functional analysis of ActVI-ORF1 reductase. *Biochemistry* **46**, 8181–8188.

Iwai Y., Kora A., Takahashi Y., Hayashi T., Awaya J., Masuma R., Oiwa R., Omura S. **(1978)** Production of deoxyfrenolicin and a new antibiotic, frenolicin B by *Streptomyces roseofulvus* strain AM-3867. *J. Antibiot. (Tokyo)* **31**, 959–965.

Javidpour P., Korman T.P., Shakya G., Tsai S.C. **(2011)** Structural and biochemical analyses of regio- and stereospecificities observed in a type II polyketide ketoreductase. *Biochemistry* **50**, 4638–4649.

Johnson L.E., Dietz A. **(1968)** Kalafungin, a new antibiotic produced by *Streptomyces tanashiensis* strain Kala. *Appl. Microbiol.* **16**, 1815–1821.

Kallio P., Sultana A., Niemi J., Mäntsälä P., Schneider G. **(2006)** Crystal structure of the polyketide cyclase AknH with bound substrate and product analogue: implications for catalytic mechanism and product stereoselectivity. *J. Mol. Biol*. **357**, 210–220.

Kasai M., Shirahata K., Ishii S., Mineura K., Marumo H., Tanaka H., Omura S. **(1979)** Structure of nanaomycin E, a new nanaomycin. *J. Antibiot. (Tokyo)* **32**, 442–445.

Keatinge-Clay A.T., Maltby D.A., Medzihradszky K.F., Khosla C., Stroud R.M. **(2004)** An antibiotic factory caught in action. *Nat. Struct. Mol. Biol.* **11**, 888–893.

Keller N.P., Turner G., Bennett J.W. **(2005)** Fungal secondary metabolism – from biochemistry to genomics. *Nat. Rev. Microbiol.* **3**, 937–947.

Kendrew S.G., Hopwood D.A., Marsh E.N. **(1997)** Identification of a monooxygenase from *Streptomyces coelicolor* A3(2) involved in biosynthesis of actinorhodin: purification and characterization of the recombinant enzyme. *J. Bacteriol.* **179**, 4305–4310.

Kharel M.K., Rohr J. **(2012)** Delineation of gilvocarcin, jadomycin, and landomycin pathways through combinatorial biosynthetic enzymology. *Curr. Opin. Chem. Biol.* **16**, 150–161.

Khosla C. **(2009)** Structures and Mechanisms of Polyketide Synthases. *J. Org. Chem.* **74**, 6416–6420.

Kieser T., Bibb M.J., Buttner M.J., Chater K.F., Hopwood D.A. **(2000)** Practical Streptomyces genetics. The John Innes Foundation, Norwich, England.

Korman T.P., Hill J.A., Vu T.N., Tsai S.C. **(2004)** Structural analysis of actinorhodin polyketide ketoreductase: cofactor binding and substrate specificity. *Biochemistry* **43**, 14529–14538.

Korman T.P., Tan Y.H., Wong J., Luo R., Tsai S.C. **(2008)** Inhibition kinetics and emodin cocrystal structure of a type II polyketide ketoreductase. *Biochemistry* **47**, 1837–1847.

Kren V., Martínková L. **(2001)** Glycosides in medicine: "The role of glycosidic residue in biological activity". *Curr. Med. Chem.* **8**, 1303–1328.

Kuck D., Caulfield T., Lyko F., Medina-Franco J.L. **(2010)** Nanaomycin A selectively inhibits DNMT3B and reactivates silenced tumor suppressor genes in human cancer cells. *Mol. Cancer. Ther.* **9**, 3015–3023.

Levin I., Miller M.D., Schwarzenbacher R., McMullan D., Abdubek P., Ambing E., Biorac T., Cambell J., Canaves J.M., Chiu H.J., Deacon A.M., DiDonato M., Elsliger M.A., Godzik A., Grittini C., Grzechnik S.K., Hale J., Hampton E., Han G.W., Haugen J., Hornsby M. Jaroszewski L., Karlak

C., Klock H.E., Koesema E., Kreusch A., Kuhn P., Lesley S.A., Morse A., Moy K., Nigoghossian E., Ouyang J., Page R., Quijano K. Reyes R., Robb A., Sims E., Spraggon G., Stevens R.C., van den Bedem H. Velasquez J., Vincent J. Wang X., West B., Wolf G., Xu Q., Zagnitko O., Hodgson K.O., Wooley J., Wilson I.A. **(2005)** Crystal structure of an indigoidine synthase A (IndA)-like protein (TM1464) from *Thermotoga maritima* at 1.90 Å resolution reveals a new fold. *Proteins* **59**, 864–868.

Li A., Itoh T., Taguchi T., Xiang T., Ebizuka Y., Ichinose K. **(2005)** Functional studies on a ketoreductase gene from *Streptomyces* sp. AM-7161 to control the stereochemistry in medermycin biosynthesis. *Bioorg. Med. Chem.* **13**, 6856–6863.

Li Q., Khosla C., Puglisi J.D., Liu C.W. **(2003)** Solution Structure and Backbone Dynamics of the Holo Form of the Frenolicin Acyl Carrier Protein. *Biochemistry* **42**, 4648–4657.

Lu Y.-W., San Roman A.K., Gehring A.M. **(2008)** Role of phosphopantetheinyl transferase genes in antibiotic production by *Streptomyces coelicolor*. *J. Bacteriol.* **190**, 6903–6908.

Malpartida F., Hopwood D.A. **(1984)** Molecular cloning of the whole biosynthetic pathway of a Streptomyces antibiotic and its expression in a heterologous host. *Nature* **309**, 462–464.

Marti T., Hu Z., Pohl N.L., Shah A.N., Khosla C. **(2000)** Cloning, nucleotide sequence, and heterologous expression of the biosynthetic gene cluster for R1128, a non-steroidal estrogen receptor antagonist. Insights into an unusual priming mechanism. *J. Biol. Chem.* **275**, 33443–33448.

Matharu A.L., Cox R.J., Crosby J., Byrom K.J., Simpson T.J. **(1998)** MCAT is not required for in vitro polyketide synthesis in a minimal actinorhodin polyketide synthase from *Streptomyces coelicolor*. *Chem. Biol.* **5**, 699–711.

McDaniel R., Ebert-Khosla S., Fu H., Hopwood D.A., Khosla C. **(1994)** Engineered biosynthesis of novel polyketides: influence of a downstream enzyme on the catalytic specificity of a minimal aromatic polyketide synthase. *Proc. Natl. Acad. Sci. U. S. A.* **91**, 11542–11546.

McDaniel R., Ebert-Khosla S., Hopwood D.A., Khosla C. **(1993)** Engineered biosynthesis of novel polyketides. *Science* **262**, 1546–1550.

Mittler M., Bechthold A., Schulz G.E. **(2007)** Structure and action of the C–C bond-forming glycosyltransferase UrdGT2 involved in the biosynthesis of the antibiotic urdamycin. *J. Mol. Biol.* **372**, 67–76.

Nakagawa A., Fukamachi N., Yamaki K., Hayashi M., Oh-ishi S., Kobayashi B., Omura S. **(1987)** Inhibition of platelet aggregation by medermycin and it's related isochromanequinone antibiotics. *J. Antibiot. (Tokyo)* **40**, 1075–1076.

Naruse N., Goto M., Watanabe Y., Terasawa T., Dobashi K. **(1998)** K1115 A, a new anthraquinone that inhibits the binding of Activator Protein-1 (AP-1) to its recognition sites. II. Taxonomy, fermentation, isolation, physico-chemical properties and structure determination. *J. Antibiot. (Tokyo)* **51**, 545–552.

O'Connor S. **(2004)** Aureolic acids: similar antibiotics with different biosynthetic gene clusters. *Chem. Biol.* **11**, 8–10.

Oja T., Tähtinen P., Dreiack N., Mäntsälä P., Niemi J., Metsä-Ketelä M., Klika K.D. **(2012)** Alnumycins A2 and A3: new inverse-epimeric pairs stereoisomeric to alnumycin A1. *Tetrahedron: Asymmetry* **23**, 670–682.

Okamoto S., Taguchi T., Ochi K., Ichinose K. **(2009)** Biosynthesis of actinorhodin and related antibiotics: discovery of alternative routes for quinone formation encoded in the *act* gene cluster. *Chem. Biol.* **16**, 226–236.

Omura S., Tsuzuki K., Iwai Y., Kishi M., Watanabe S., Shimizu H. **(1985)** Anticoccidial activity of frenolicin B and its derivatives. *J. Antibiot. (Tokyo)* **38**, 1447–1448.

Pan H., Tsai S., Meadows E.S., Miercke L.J., Keatinge-Clay A.T., O'Connell J., Khosla C., Stroud R.M. **(2002)** Crystal structure of the priming beta-ketosynthase from the R1128 polyketide biosynthetic pathway. *Structure* **10**, 1559–1568.

Preumont A., Snoussi K., Stroobant V., Collet J.F., Van Schaftingen E. **(2008)** Molecular identification of pseudouridine-metabolizing enzymes. *J. Biol. Chem.* **283**, 25238–25246.

Rutherford K., Parkhill J., Crook J., Horsnell T., Rice P., Rajandream M.A., Barrell B. **(2000)** Artemis: sequence visualization and annotation. *Bioinformatics* **16**, 944–945.

Salaski E.J., Krishnamurthy G., Ding W.-D., Yu K., Insaf S.S., Eid C., Shim J., Levin J.I., Tabei K., Toral-Barza L., Zhang W.-G., McDonald L.A., Honores E., Hanna C., Yamashita A., Johnson B., Li Z., Laakso L., Powell D., Mansour T.S. **(2009)** Pyranonaphthoquinone lactones: a new class of AKT selective kinase inhibitors alkylate a regulatory loop cysteine. *J. Med. Chem.* **52**, 2181–2184.

Santos-Beneit F., Barriuso-Iglesias M., Fernández-Martínez L.T., Martínez-Castro M., Sola-Landa A., Rodríguez-García A., Martín J.F. **(2011)** The RNA polymerase omega factor RpoZ is regulated

by PhoP and has an important role in antibiotic biosynthesis and morphological differentiation in *Streptomyces coelicolor*. *Appl. Environ. Microbiol.* **77**, 7586–7594.

Schneider G. **(2005)** Enzymes in the biosynthesis of aromatic polyketide antibiotics. *Curr. Opin. Struct. Biol.* **15**, 629–636.

Sciara G., Kendrew S.G., Miele A.E., Marsh N.G., Federici L., Malatesta F., Schimperna G., Savino C., Vallone B. **(2003)** The structure of ActVA-Orf6, a novel type of monooxygenase involved in actinorhodin biosynthesis. *Embo J.* **22**, 205–215.

Smith S., Tsai S.C. **(2007)** The type I fatty acid and polyketide synthases: a tale of two megasynthases. *Nat. Prod. Rep.* **24**, 1041–1072.

Sun D., Hansen M., Clement J.J., Hurley L.H. **(1993)** Structure of the altromycin B (N7-guanine)-DNA adduct. A proposed prototypic DNA adduct structure for the pluramycin antitumor antibiotics. *Biochemistry* **32**, 8068–8074.

Taguchi T., Ebihara T., Furukawa A., Hidaka Y., Ariga R., Okamoto S., Ichinose K. **(2012)** Identification of the actinorhodin monomer and its related compound from a deletion mutant of the actVA-ORF4 gene of *Streptomyces coelicolor* A3(2). *Bioorg. Med. Chem. Lett*. **22**, 5041–5045.

Taguchi T., Ebizuka Y., Hopwood D.A., Ichinose K. **(2001)** A new mode of stereochemical control revealed by analysis of the biosynthesis of dihydrogranaticin in *Streptomyces violaceoruber* Tü22. *J. Am. Chem. Soc.* **123**, 11376–11380.

Taguchi T., Kunieda K., Takeda-Shitaka M., Takaya D., Kawano N., Kimberley M.R., Booker-Milburn K.I., Stephenson G.R., Umeyama H., Ebizuka Y., Ichinose K. **(2004)** Remarkably different structures and reaction mechanisms of ketoreductases for the opposite stereochemical control in the biosynthesis of BIQ antibiotics. *Bioorg. Med. Chem.* **12**, 5917–5927.

Taguchi T., Okamoto S., Hasegawa K., Ichinose K. **(2011)** Epoxyquinone formation catalyzed by a two-component flavin-dependent monooxygenase involved in biosynthesis of the antibiotic actinorhodin. *ChemBioChem* **12**, 2767–2773.

Takano E., Chakraburtty R., Nihira T., Yamada Y., Bibb M.J. **(2001)** A complex role for the γ-butyrolactone SCB1 in regulating antibiotic production in *Streptomyces coelicolor* A3(2). *Mol. Microbiol.* **41**, 1015–1028.

Takano S., Hasuda K., Ito A., Koide Y., Ishii F. **(1976)** A new antibiotic, medermycin. *J. Antibiot. (Tokyo)* **29**, 765–768.

Tanaka H., Koyama Y., Awaya J., Marumo H., Oiwa R. **(1975a)** Nanaomycins, new antibiotics produced by a strain of *Streptomyces*. I. Taxonomy, isolation, characterization and biological properties. *J. Antibiot. (Tokyo)* **28**, 860–867.

Tanaka H., Koyama Y., Nagai T., Marumo H., Omura S. **(1975b)** Nanomycins, new antibiotics produced by a strain of *Streptomyces*. II. Structure and biosynthesis. *J. Antibiot. (Tokyo)* **28**, 868–875.

Tanaka H., Marumo H., Nagai T., Okada M., Taniguchi K. **(1975c)** Nanaomycins, new antibiotics produced by a strain of *Streptomyces*. III. A new component, nanaomycin C, and biological activities of nanaomycin derivatives. *J. Antibiot. (Tokyo)* **28**, 925–930.

Tanaka H., Minami-Kakinuma S., Omura S. **(1982)** Biosynthesis of nanaomycin. III. Nanaomycin A formation from nanaomycin D by nanaomycin D reductase via a hydroquinone. *J. Antibiot. (Tokyo)* **35**, 1565–1570.

Tanaka N., Okabe T., Isono F., Kashiwagi M., Nomoto K., Takahashi M., Shimazu A., Nishimura T. **(1985)** Lactoquinomycin, a novel anticancer antibiotic. I. Taxonomy, isolation and biological activity. *J. Antibiot. (Tokyo)* **38**, 1327–1332.

Tang Y., Koppisch A.T., Khosla C. **(2004)** The acyltransferase homologue from the initiation module of the R1128 polyketide synthase is an acyl-ACP thioesterase that edits acetyl primer units. *Biochemistry* **43**, 9546–9555.

Tang Y., Lee T.S., Kobayashi S., Khosla C. **(2003)** Ketosynthases in the initiation and elongation modules of aromatic polyketide synthases have orthogonal acyl carrier protein specificity. *Biochemistry* **42**, 6588–6595.

Tatsuta K., Ozeki H., Yamaguchi M., Tanaka M., Okui T. **(1990)** Enantioselective total synthesis of medermycin (lactoquinomycin). *Tetrahedron Lett.* **31**, 5495–5498.

Tatsuta K., Ozeki H., Yamaguchi M., Tanaka M., Okui T., Nakata M. **(1991)** Total synthesis and biological evaluation of unnatural (-)-medermycin [(-)-lactoquinomycin]. *J. Antibiot. (Tokyo)* **44**, 901–902.

Tatsuta K., Tokishita S., Fukuda T., Kano T., Komiya T., Hosokawa S. **(2011)** The first total synthesis and structural determination of antibiotics K1115 B1s (alnumycins). *Tetrahedron Lett.* **52**, 983–986.

Thibodeaux C.J., Melançon C.E., Liu H.-w. **(2007)** Unusual sugar biosynthesis and natural product glycodiversification. *Nature* **446**, 1008–1016.

Toral-Barza L., Zhang W.-G., Huang X., McDonald L.A., Salaski E.J., Barbieri L.R., Ding W.-D.,

Krishnamurthy G., Hu Y.B., Lucas J., Bernan V.S., Cai P., Levin J.I., Mansour T.S., Gibbons J.J., Abraham R.T., Yu K. **(2007)** Discovery of lactoquinomycin and related pyranonaphthoquinones as potent and allosteric inhibitors of AKT/PKB: mechanistic involvement of AKT catalytic activation loop cysteines. *Mol. Cancer Ther.* **6**, 3028–3038.

Tornus D., Floss H.G. **(2001)** Identification of four genes from the granaticin biosynthetic gene cluster of *Streptomyces violaceoruber* Tü22 involved in the biosynthesis of L-rhodinose. *J. Antibiot. (Tokyo)* **54**, 91–101.

Tsuji N., Kobayashi M., Wakisaka Y., Kawamura Y., Mayama M., Matsumoto K. **(1976)** New antibiotics, griseusins A and B. Isolation and characterization. *J. Antibiot. (Tokyo)* **29**, 7–9.

Tsuzuki K., Iwai Y., Omura S., Shimizu H., Kitajima N. **(1986)** Nanaomycins production by a frenolicin B producing strain. *J. Antibiot. (Tokyo) 39*, 1343-1345.

Tähtinen P., Oja T., Dreiack N., Mäntsälä P., Niemi J., Metsä-Ketelä M., Klika K.D. **(2012)** Epimers vs. inverse epimers: the C-1 configuration in alnumycin A1. *RSC Adv.* **2**, 5098–5100.

Valton J., Fontecave M., Douki T., Kendrew S.G., Niviere V. **(2006)** An aromatic hydroxylation reaction catalyzed by a two-component FMN-dependent Monooxygenase. The ActVA-ActVB system from *Streptomyces coelicolor*. *J. Biol. Chem.* **281**, 27–35.

Valton J., Mathevon C., Fontecave M., Nivière V., Ballou D.P. **(2008)** Mechanism and regulation of the two-component FMN-dependent monooxygenase ActVA-ActVB from *Streptomyces coelicolor*. *J. Biol. Chem.* **283**, 10287–10296.

van Wezel G.P., McDowall K.J. **(2011)** The regulation of the secondary metabolism of Streptomyces: new links and experimental advances. *Nat. Prod. Rep.* **28**, 1311–1333.

Volkmann C., Zeeck A., Potterat O., Zähner H., Bohnen F.M., Herbst-Irmer R. **(1995)** Metabolic products of microorganismen. 270. The structures of the exfoliamycins. *J. Antibiot. (Tokyo)* **48**, 431–432.

Watanabe K., Praseuth A.P., Wang C.C. **(2007)** A comprehensive and engaging overview of the type III family of polyketide synthases. *Curr. Opin. Chem. Biol.* **11**, 279–286.

Weymouth-Wilson A.C. **(1997)** The role of carbohydrates in biologically active natural products. *Nat. Prod. Rep.* **14**, 99–110.

White S.W., Zheng J., Zhang Y.M., Rock C.O. **(2005)** The structural biology of type II fatty acid biosynthesis. *Annu. Rev. Biochem.* **74**, 791–831.

Willems A.R., Tahlan K., Taguchi T., Zhang K., Lee Z.Z., Ichinose K., Junop M.S., Nodwell J.R. **(2008)** Crystal structures of the *Streptomyces coelicolor* TetR-like protein ActR alone and in complex with actinorhodin or the actinorhodin biosynthetic precursor (S)-DNPA. *J. Mol. Biol.* **376**, 1377–1387.

Wright L.F., Hopwood D.A. **(1976)** Actinorhodin is a chromosomally-determined antibiotic in *Streptomyces coelicolar* A3(2). *J. Gen. Microbiol.* **96**, 289–297.

Xu Z., Metsä-Ketelä M., Hertweck C. **(2009)** Ketosynthase III as a gateway to engineering the biosynthesis of antitumoral benastatin derivatives. *J. Biotechnol.* **140**, 107–113.

Xu Z., Schenk A., Hertweck C. **(2007)** Molecular analysis of the benastatin biosynthetic pathway and genetic engineering of altered fatty acid–polyketide hybrids. *J. Am. Chem. Soc.* **129**, 6022–6030.

Ylihonko K., Hakala J., Niemi J., Lundell J., Mäntsälä P. **(1994)** Isolation and characterization of aclacinomycin A-non-producing *Streptomyces galilaeus* (ATCC 31615) mutants. *Microbiology* **140**, 1359–1365.

Yu T.W., Bibb M.J., Revill W.P., Hopwood D.A. **(1994)** Cloning, sequencing, and analysis of the griseusin polyketide synthase gene cluster from *Streptomyces griseus*. *J. Bacteriol.* **176**, 2627–2634.

Yunt Z., Reinhardt K., Li A., Engeser M., Dahse H.M., Gütschow M., Bruhn T., Bringmann G., Piel J. **(2009)** Cleavage of four carbon–carbon bonds during biosynthesis of the griseorhodin a spiroketal pharmacophore. *J. Am. Chem. Soc.* **131**, 2297–2305.

Zeeck A., Mardin M. **(1974)** Stoffwechselprodukte von Mikroorganismen, 1281) Isolierung und Konstitution von α-Naphthocyclinon. *Justus Liebigs Ann. Chem.* **1974**, 1063–1099.

Zhou H., Li Y., Tang Y. **(2010)** Cyclization of aromatic polyketides from bacteria and fungi. *Nat. Prod. Rep.* **27**, 839–868.